



ARTICLE

Calorie restriction activates a gastric Notch-FOXO1 pathway to expand ghrelin cells

Wendy M. McKimpon^{1,2} , Sophia Spiegel^{1,2} , Maria Mukhanova^{1,2} , Michael Kraakman^{1,2} , Wen Du^{1,2} , Takumi Kitamoto^{1,2} , Junjie Yu^{1,2} , Zhaobin Deng^{1,2} , Utpal Pajvani^{1,2} , and Domenico Accili^{1,2} 

Calorie restriction increases lifespan. Among the tissue-specific protective effects of calorie restriction, the impact on the gastrointestinal tract remains unclear. We report increased numbers of chromogranin A-positive (+), including orexigenic ghrelin+ cells, in the stomach of calorie-restricted mice. This effect was accompanied by increased Notch target Hes1 and Notch ligand Jag1 and was reversed by blocking Notch with DAPT, a gamma-secretase inhibitor. Primary cultures and genetically modified reporter mice show that increased endocrine cell abundance is due to altered Lgr5+ stem and Neurog3+ endocrine progenitor cell proliferation. Different from the intestine, calorie restriction decreased gastric Lgr5+ stem cells, while increasing a FOXO1/Neurog3+ subpopulation of endocrine progenitors in a Notch-dependent manner. Further, activation of FOXO1 was sufficient to promote endocrine cell differentiation independent of Notch. The Notch inhibitor PF-03084014 or ghrelin receptor antagonist GHRP-6 reversed the phenotypic effects of calorie restriction in mice. Tirzepatide additionally expanded ghrelin+ cells in mice. In summary, calorie restriction promotes Notch-dependent, FOXO1-regulated gastric endocrine cell differentiation.

Introduction

Restricting calories can extend lifespan (McCay et al., 1989) in humans, as well as other species (Weindruch et al., 1986). Calorie restriction also improves health by delaying the onset of age-related diseases including degenerative brain disease, heart disease, type 2 diabetes, and certain types of cancer (Colman et al., 2009; Madeo et al., 2019). The mechanism of the alleged protective effect of calorie restriction is unknown. Interestingly, energy expenditure and oxidative stress markers decrease in humans who restricted their diet by 15% over a 2-year period (Il'yasova et al., 2018; Redman et al., 2018). Cardiometabolic risk factors (Most et al., 2018) and circulating tumor necrosis factor- α (Ravussin et al., 2015), a marker of inflammation, also show a similar pattern.

Epithelial cell types have specialized functions. Distinct processes of the gastrointestinal (GI) tract, such as the absorption of lipids and nutrients, are driven, in part, by distinct subtypes of epithelial cells, which are repopulated by stem and progenitor cells, including Lgr5 multipotent stem cells in the intestine (Barker et al., 2007) and antral stomach (Barker et al., 2010).

Enteroendocrine cells located throughout the gut sense nutrients and release hormones that regulate food intake and

satiety (Gribble and Reimann, 2016). These cells are distributed along the GI tract in a region-specific manner (Thompson et al., 2018). For example, intestinal K- and L- cells, which produce the gut incretins GIP and GLP-1 respectively, are enriched in the upper and lower intestines, respectively (Baggio and Drucker, 2007). On the other hand, the hormone ghrelin, released during food restriction to increase food intake (Kojima et al., 1999), is most prominently produced by gastric epithelial cells (Drucker, 2007). Mechanisms that drive this regional specificity in the distribution of enteroendocrine subtypes are not clear but likely involve differentiation of stem cells, such as Lgr5+ cells, and endocrine progenitor cells, marked by the transcription factor Neurogenin3 (Neurog3).

The gastrointestinal tract is affected by calorie restriction. Interestingly, in the small intestine, calorie restriction expands crypt size, while decreasing villi length (Yilmaz et al., 2012). In addition, it decreases the number of different cell types, including chromogranin A+ enteroendocrine cells, while increasing the proliferation of Lgr5+ stem cells (Igarashi and Guarente, 2016). Fasting also promotes fatty acid oxidation within intestinal stem cells (Mihaylova et al., 2018). The role of Lgr5+ stem

¹Department of Medicine, Division of Endocrinology, Columbia University, New York, NY, USA; ²Naomi Berrie Diabetes Center, Columbia University, New York, NY, USA.

Correspondence to Wendy M. McKimpon: wm2347@cumc.columbia.edu, wmckimp@gmail.com

J. Yu's current affiliation is Institute of Pharmaceutical Sciences, China Pharmaceutical University, Nanjing, China.

© 2024 McKimpon et al. This article is distributed under the terms of an Attribution-Noncommercial-Share Alike-No Mirror Sites license for the first six months after the publication date (see <http://www.rupress.org/terms/>). After six months it is available under a Creative Commons License (Attribution-Noncommercial-Share Alike 4.0 International license, as described at <https://creativecommons.org/licenses/by-nc-sa/4.0/>).

cells in antral gastric tissue (Barker et al., 2010) upon calorie restriction has not been studied.

Distinct programs are activated by calorie restriction in each organ. For example, high-throughput transcriptomic, proteomic, and metabolomic analyses of the liver found that calorie restriction induces RNA processing (Rhoads et al., 2018). In contrast, it triggers remodeling of skin and fur (Forni et al., 2017). Less is known about how calorie restriction impacts stomach cells, although ghrelin levels reportedly increase (Reimer et al., 2010). It has also recently come to light that cells in each tissue have a unique transcription network to regulate the reversal of age-related gene expression changes by calorie restriction (Ma et al., 2020).

Herein, we report that calorie restriction initiates a distinct gastric program affecting stem and endocrine progenitors in the stomach by modulating Notch activity. Further, during calorie restriction, the transcription factor FOXO1 preferentially undergoes nuclear translocation in gastric endocrine progenitor cells to trigger an increase in ghrelin+ cells, thereby stimulating food intake.

Results

Calorie restriction alters gastric endocrine cell composition

Plasma ghrelin increases after calorie restriction (Reimer et al., 2010). To investigate whether this is due to increased ghrelin cell number, we calorie-restricted female mice by 30% of their daily food intake (CR) for 4 wk and assessed the abundance of gastric cell populations after food restriction. Controls had unlimited access to food (ad libitum) during this time. After calorie restriction, wild-type female CR mice showed decreased weight (Fig. 1 A), lean mass (Fig. 1 B), and fed glucose (Fig. 1 C) compared with controls. The latter gained weight, as expected (Fig. 1 A). A similar decrease in body weight (Fig. S1, A, C, D, and E; and Fig. 1 E), lean mass (Fig. S1, B, F, G, and H; and Fig. 1 H), and fasting glucose (Fig. S1 I) was seen in a second cohort of female FOXO1-Venus (FoxV) knock-in reporter mice (Kuo et al., 2019).

We analyzed the stomach of these mice in the corpus, composed of gastric oxyntic glands that contain acid-secreting parietal cells to aid in food digestion, and the antrum, which funnels digested food into the intestine for further processing. The glandular epithelium of the antral stomach contains gastrin-secreting endocrine cells, but not (in mouse tissue) parietal cells. Interestingly, when we assessed ghrelin+ cell number by immunostaining, we found a doubling of cell abundance in both antrum and corpus (Fig. 1 D and Fig. S2 A).

In contrast, other endocrine cell populations positive for 5HT and gastrin were unaltered (Fig. 1, E and F; and Fig. S2, B and C). We saw a slight but significant increase in glucagon cells (Fig. 1 G and Fig. S2 D). We next examined alterations in differentiated endocrine cells after calorie restriction using general endocrine cell markers. While the number of synaptophysin+ cells did not change, we found a significant increase of chromogranin A+ cells in the antrum (AL: 4.2% versus CR: 7.8%) and corpus (AL: 5.8% versus CR: 9.1%) (Fig. 1 H and Fig. S2 E).

To determine whether these changes were dependent on biological sex, we calorie-restricted male mice by 30% over 4 wk. At the end, animals had lower body weight (Fig. 1 I), lean mass

(Fig. 1 J), and fed glucose (Fig. 1 K) compared to male mice fed ad libitum. Similar to female mice, males also had more ghrelin+ cells in both antrum (AL: 0.8% versus CR: 1.8%) and corpus (AL: 1.1% versus CR: 2.2%) (Fig. 1 L and Fig. S3 A). This corresponded with an increase in chromogranin A+ endocrine cells from 1.8 to 4.2% in the antrum and 3.4–5.7% in the corpus (Fig. 1 M and Fig. S3 B).

Gastric notch signaling is triggered by food restriction

We recapitulated these changes ex vivo by culturing primary stomach cultures (PSC) in a serum-deprived medium. The abundance of ghrelin+ cells in PSC increased from 1.6% in normal medium to 3.8% when grown in serum-deprived medium (Fig. 2 A). Similarly, chromogranin A+ cells also increased from 3.8 to 9.0% with serum deprivation (Fig. 2 A).

To determine the signaling mechanisms regulating these changes in endocrine cell abundance, we surveyed molecular pathways involved in gastric cell differentiation. We found a substantial increase in cells positive for the Notch transcriptional target *Hes1* after serum deprivation, consistent with increased Notch activity (Fig. 2 B). Importantly, we also saw increased Notch ligand levels under the same conditions (Fig. 2, B and D).

To test whether the increase in Notch-active cells with serum deprivation was linked to the increased ghrelin cells, we blocked Notch signaling in PSC with the γ -secretase inhibitor DAPT (Fig. 2 C). DAPT treatment diminished the increased *Jag1* mRNA in serum-deprived PSC (Fig. 2 D). Interestingly, the increased number of ghrelin+ cells in PSC caused by serum deprivation was reversed by overnight treatment with DAPT (Fig. 2 E). Conversely, cre recombination-mediated expression of the Notch intracellular domain (NICD) triggered an increase of chromogranin A-immunoreactive cells under control (7.5 versus 3.2%) and serum-deprived (17.7 versus 10.4%) conditions (Fig. 2 F). Cells overexpressing NICD, identified by cre activation of a fluorescence Tomato reporter, also contained increased *chromogranin A* (7.93 ± 2.03 versus 1.08 ± 0.28) and *ghrelin* (3.21 ± 0.96 versus 0.55 ± 0.18) mRNA (Fig. 2 G). Adenoviral-mediated expression of NICD-GFP increased the propensity of cells to differentiate into ghrelin+ cells fourfold (Fig. 2 H). These data suggest that activation of Notch signaling is necessary and sufficient to increase chromogranin A+ and ghrelin+ cells during calorie restriction.

Active notch perturbs gastric stem cells

Notch signaling regulates gastric *Lgr5* stem cell differentiation (Demitrack et al., 2015). To determine if changes in differentiated endocrine cells were due to changes in *Lgr5*+ stem and *Neurog3*+ progenitor populations, we calorie-restricted *Lgr5*-GFP and *Neurog3*-GFP knock-in reporter mice. In the stomach, the former reporter labels a population of self-renewing, multipotent antral stem cells that maintain gastric epithelial cell homeostasis (Barker et al., 2010), whereas the latter marks *Neurog3*+ endocrine progenitor cells that differentiate into endocrine cells (Schonhoff et al., 2004). These reporter mice had lower glucose levels (Fig. 3 A) and decreased lean mass (Fig. 3 B) upon calorie restriction. In the stomach, calorie restriction triggered a decrease in antral *Lgr5*-GFP+ cells (Fig. 3, C and D). In

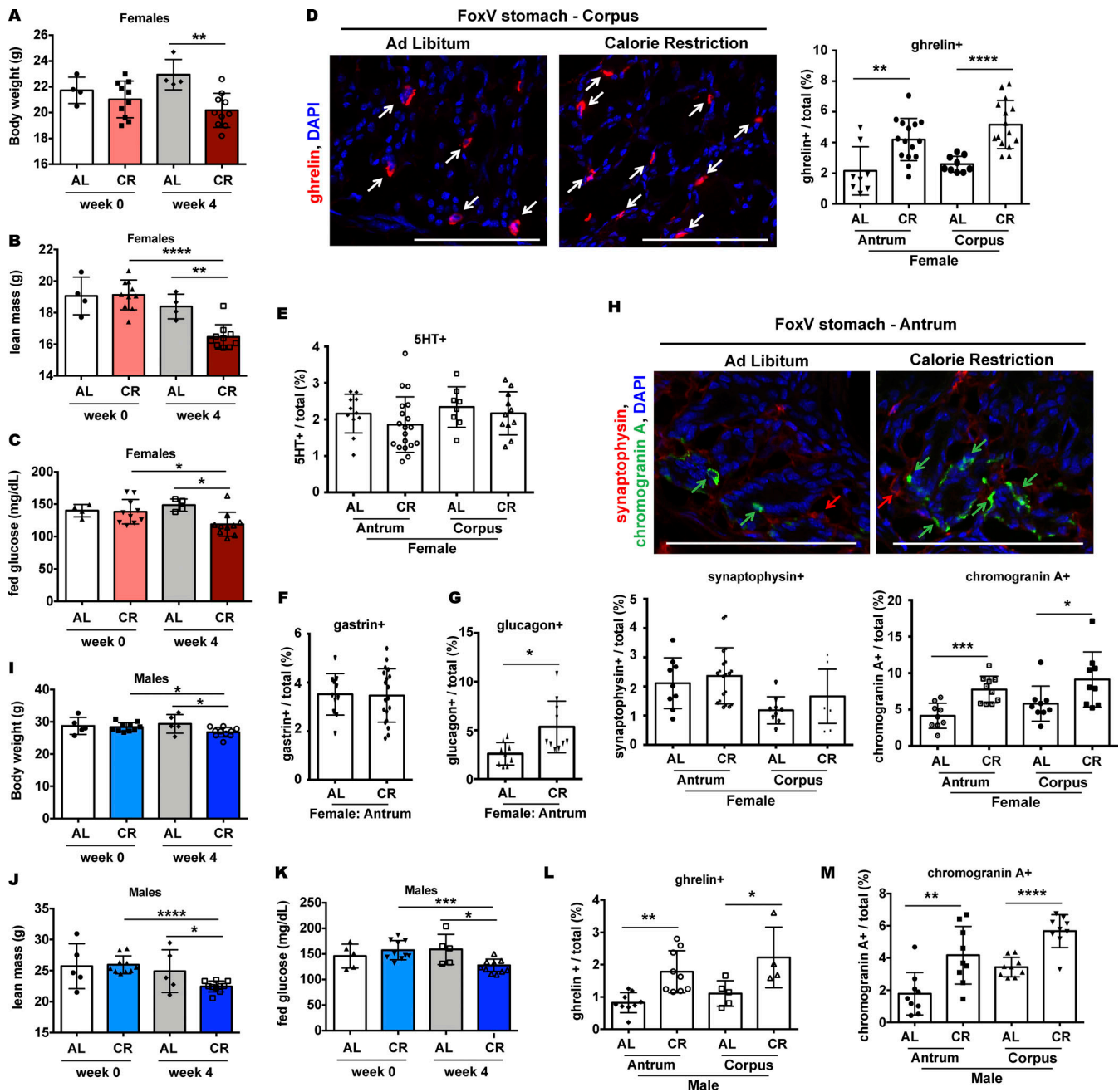


Figure 1. **Gastric endocrine cells become more abundant after calorie restriction.** (A) Body weight after female wild-type mice were fed ad libitum (AL, $n = 4$ mice) or 30% food restricted (CR, $n = 10$ mice) for 4 wk. Mice were 14 wk of age at the start of calorie restriction. (B) Lean mass measurements in AL and CR mice. (C) Fed blood glucose measurements in AL and CR mice. (D) Representative fluorescent staining (left) with quantification (right) of ghrelin-expressing cells in stomach tissue from AL and CR mice. Tissue is from a second cohort of female FOXO1-Venus (FoxV) reporter mice calorie restricted (at 12 wk old) by 30% for 4 wk. Metabolic data for these mice are displayed in Fig. S1. (E–G) Quantification of specific endocrine cell populations in female AL and CR FoxV stomach. Lower magnification images of general and specific endocrine cell markers, in antrum and corpus stomach tissue, are displayed in Fig. S2. (H) Fluorescent staining (top) with quantification (bottom) for general endocrine markers synaptophysin (red) and chromogranin A (green) in female AL and CR stomach tissue. (I–K) Body weight (I), lean mass (J), and fed glucose (K) measurements in male mice fed ad libitum (AL, $n = 5$ mice) or 30% food restricted (CR, $n = 10$ mice) for 4 wk. Mice were 14 wk of age at the start of calorie restriction. (L and M) Quantification of ghrelin (L) and chromogranin A (M) staining in stomach tissue of AL and CR male mice. Representative lower magnification images of staining in a second independent cohort of male CR mice are displayed in Fig. S3. Arrows denote ghrelin+ (white), chromogranin A+ (green), and synaptophysin+ (red) cells. Scale bar is 100 μm . DAPI counterstains nuclei. For each cell marker, percentage positive cells represent the number of immunoreactive+ cells/DAPI+ nuclei per microscope field. Bar graphs show mean \pm standard deviation. Each dot represents values from individual mouse (A–C, and I–K) or quantification of a microscopic field (D–H, L, and M) from AL and CR mice as indicated. * $P < 0.05$, ** $P < 0.01$, *** $P < 0.001$, and **** $P < 0.0001$.

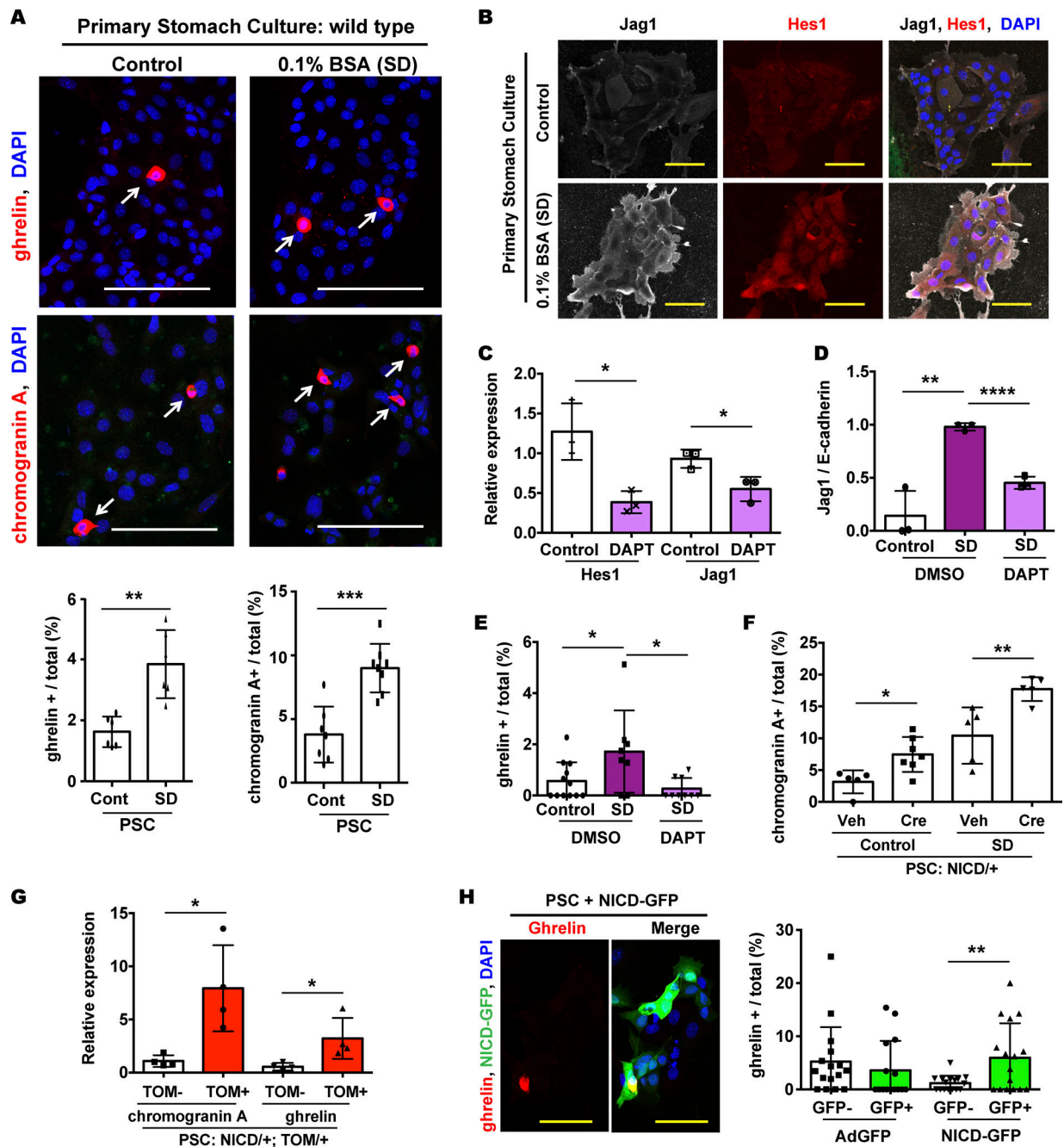


Figure 2. **Serum deprivation in primary culture activates notch signaling to increase ghrelin+ cells.** (A) Immunohistochemistry (top) with quantification (bottom) of primary stomach cultures (PSC) generated from wild-type mice and cultured in control and serum-deprived (SD; 0.1% BSA) media stained for endocrine markers. (B) Immunohistochemistry of wild type PSC cultured in control or SD media stained for Notch ligand Jag1 and Notch transcription factor Hes1. (C) Gene expression of PSC after overnight treatment with γ -secretase inhibitor DAPT (10 μ M). (D) Jag1 expression in PSC grown with control, SD (0.1% BSA) media, or SD media treated with DAPT. (E) Quantification of ghrelin immunohistochemistry of wild-type PSC grown in control, SD, or SD + DAPT media. (F) Quantification of chromogranin A staining in PSC generated from NICD+/+ mice and treated with vehicle (Veh) or 4 μ M recombinant TAT-cre (Cre) for 1 day. PSC were stained following an overnight recovery after Cre treatment. (G) Gene expression of Tomato (TOM)- (white bars) and TOM+ (red bars) cells purified by FACS. PSC analyzed were from NICD+/+; TOM+/+ mice and treated overnight with Cre to induce NICD. Cells collected were either negative (TOM-) or positive (TOM+) for endogenous tomato, which fluoresces upon cre recombination. (H) Representative image (left) with quantification (right) of wild-type primary stomach cultures transduced overnight with control (AdGFP) or NICD (NICD-GFP) adenovirus and then immunostained for Ghrelin. White scale bar is 100 μ m, yellow scale bar is 50 μ m. White arrow denotes a positive cell. DAPI counterstains nuclei. For each cell marker, percentage positive cells represent the number of immunoreactive+ cells/DAPI+ nuclei per microscope field. Gene expression is normalized to *E-cadherin* (C and D) or *GAPDH* (G). Bar graphs show mean \pm standard deviation. Each dot represents quantification of a microscopic field from PSC (A, E, F, and H) or independent sample of PSC for gene expression analysis (C, D, and G). *P < 0.05, **P < 0.01, ***P < 0.001, ****P < 0.0001.

contrast, cells that express transcription factor Sox2, another marker of multipotent stomach stem cells (Arnold et al., 2011), increased in the stomach and corpus (Fig. 3 E).

To test the involvement of Notch signaling in stem cell maintenance after calorie restriction, we used PSC. Serum-deprived PSC isolated from Lgr5-GFP mice had 40% fewer Lgr5-GFP+ cells compared with the serum-containing medium (Fig. 3 F). This decrease was dependent upon Notch activation, as treatment with DAPT restored Lgr5-GFP+ cell number (Fig. 3 F). To determine which cells activated Notch in response to food restriction, we immunostained Lgr5-GFP CR stomach tissue. Interestingly, there was a broad increase in Hes1 and Jag1 abundance throughout the entire antral gastric epithelial with calorie restriction, indicating that Notch is also activated outside of the Lgr5-GFP stem cells themselves (Fig. 3, G and H).

Notch promotes expansion of FOXO1+, Neurog3+ endocrine progenitors

Using the calorie-restricted reporter mice described above (Fig. 3, A and B), we next analyzed endocrine progenitor cell populations. Neurog3-GFP+ endocrine progenitor cells increased, particularly in the antral stomach, after calorie restriction (Fig. 4, A and B). Similar to in vivo, PSC grown in a serum-deprived medium increased Neurog3-GFP+ cells by 180% as detected by immunohistochemistry (Fig. 4, C and D). This increased abundance was reversed when cultures were treated with the Notch inhibitor, DAPT (Fig. 4, C and D). Serum deprivation also increased the abundance of Neurog3-GFP+ cells ($0.58\% \pm 0.031$ versus $0.47\% \pm 0.01$) as detected by endogenous fluorescence using FACS (Fig. 4, E and F). Neurog3-GFP+ cells were enriched for *Neurog3* mRNA, confirming the identity of the cell population (Fig. 4 G). Upon further analysis, *Hes1* mRNA was also increased in serum-deprived Neurog3-GFP+ cells, indicating Notch activation in these cells (Fig. 4 H). Similar to previous reports (McKimpson et al., 2022; Talchai et al., 2012), Neurog3-GFP+ cells were also enriched for FOXO1 (Fig. 4 I). Interestingly, FOXO1 mRNA was further increased in Neurog3-GFP cells grown under serum-deprived conditions (Fig. 4 I).

Given the change in FOXO1 levels, we next analyzed the effect of calorie restriction on FOXO1-expressing cells in the stomach. To detect FOXO1, we used GFP immunohistochemistry in FoxV reporter mice (McKimpson et al., 2022) (denoted as FOXO1-GFP), with pancreatic islets acting as a positive control (Fig. S4 A). No reactivity was detected in wild-type mice (Figure S4 B). Immunohistochemistry revealed that stomachs of calorie-restricted mice had ~135% more FOXO1-GFP+ cells in the antrum (Fig. 5, A and B), with some regions of FoxV CR mice having significantly more FOXO1-GFP+ cells (Fig. 5 C). There were also ~170% more FOXO1-GFP+ cells in the corpus of FoxV CR mice (Fig. 5, D and E).

Changes in cell number can be due to proliferation. Interestingly, under basal conditions, FOXO1-positive stomach cells are minimally proliferative, as indicated by the paucity of FOXO1-GFP+ cells colocalizing with proliferation markers phosphohistone H3 (pHH3) (Fig. 5 F) and Ki67 (Fig. 5 G). However, there was a significant 195% increase in FOXO1-expressing GFP+, pHH3+ cells after calorie restriction (Fig. 5 H). FOXO1-expressing

Neurog3+ cells also increased after calorie restriction (Fig. 5, I and J).

Nuclear FOXO1 triggers an increase in Ghrelin+ cells

In ad libitum-fed conditions, FOXO1 is mainly detected in the cytoplasm of gastric cells by immunohistochemistry (McKimpson et al., 2022). However, FOXO1 actively translocates between the cytoplasm and the nucleus, the latter where it drives the expression of key transcriptional targets. To test the role of nuclear FOXO1 in gastric endocrine cell remodeling following calorie restriction, we studied PSC from knock-in mice homozygous for a constitutively nuclear acetylation-defective FOXO1 (FoxKR) (Banks et al., 2011). On C57BL/6 background, FoxKR mice display glucose and insulin levels similar to control mice and have lower plasma and hepatic triglyceride levels (Qiang et al., 2012). As expected, *Foxo1* mRNA levels were similar in PSC from wild-type and FoxKR mice (Fig. 6 A). While expression of different stomach cell markers, including *Lgr5* and *Neurog3*, were minimally altered under ad libitum-fed conditions, *ghrelin* mRNA levels (1.97 ± 0.18 in FoxKR versus 0.85 ± 0.13 in wild type) were significantly increased in FoxKR PSC (Fig. 6 A), as were Ghrelin+ cells (3.30% in FoxKR versus 0.71% in wild type) (Fig. 6 B).

We confirmed these results by immunohistochemistry of stomach sections. FOXO1 was nuclear in FoxKR mice (Fig. 6 C). While the number of ghrelin+ cells in the antrum of these mice was slightly changed from controls, there was a striking increase in ghrelin+ cells in the corpus (6.20% in FoxKR versus 2.58% in wild type) (Fig. 6, D and E). In line with ghrelin being an orexigenic hormone, FoxKR mice also had increased food intake (Fig. 6 F). Furthermore, treatment of serum-deprived PSC overnight with a FOXO1 inhibitor (compound 10 [Langlet et al., 2017]) reversed the increased abundance of ghrelin+ (Fig. 6 G) and chromogranin A+ (Fig. 6 H) cells under these culture conditions. Taken together, our results suggest a role for nuclear FOXO1 in promoting the differentiation of ghrelin+ cells with calorie restriction.

To test whether the role of FOXO1 was dependent on Notch signaling, we treated PSC from wild-type and FoxKR mice with the Notch inhibitor DAPT and measured chromogranin A+ and ghrelin+ cells by immunohistochemistry (Fig. 6 I). PSC generated from FoxKR stomachs had an increased number of ghrelin+ cells (3.3%) compared with ghrelin+ cells in wild-type PSC (1.4%) (Fig. 6 J). In PSC from wild-type mice, ghrelin+ cells increased to 2.8% upon serum deprivation and this was reversed to 1.2% by DAPT treatment. Neither treatment affected the number of ghrelin+ (Fig. 6 J) or chromogranin A+ (Fig. 6 K) cells in FoxKR PSC. We also assessed Notch signaling in wild-type and FoxKR stomach. Expression of Notch components *Hes1* and *Jag1* was similar in the antrum and corpus from both genotypes (Fig. 6, L and M). These data link nuclear FOXO1 with ghrelin cell differentiation downstream of Notch activation.

A physiological role for the induction of ghrelin+ cells

Similar to another report (Reimer et al., 2010), we found increased plasma ghrelin levels in calorie-restricted mice (Fig. 7, A and B). This increase occurred when either female (Fig. 7 A) or

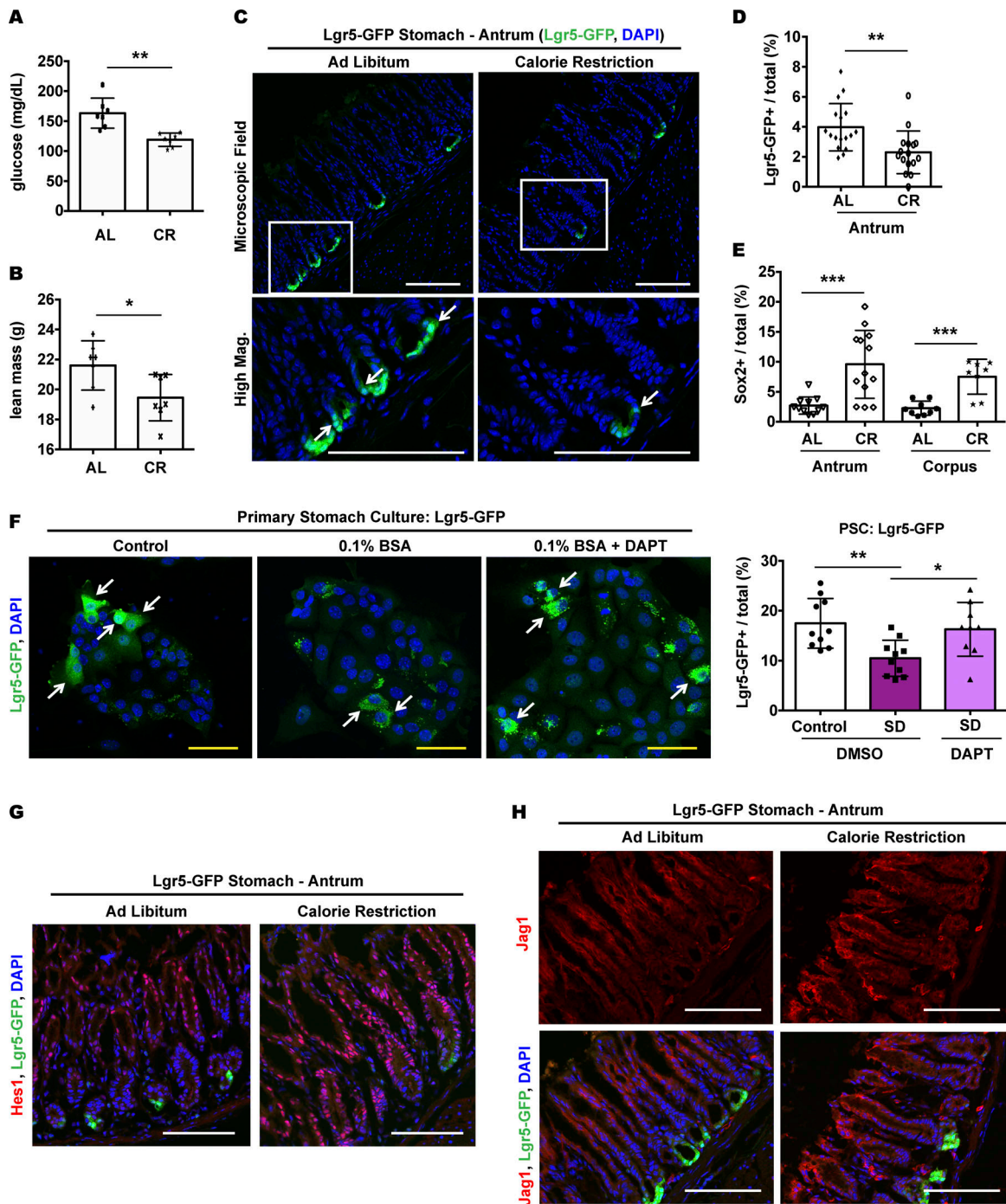


Figure 3. Calorie restriction decreases the number of gastric Lgr5+ stem cells in a notch-dependent manner. (A) Fed blood glucose measurements after Lgr5-GFP and Neurog3-GFP reporter mice were fed ad libitum (AL) or 30% food restricted (CR) for 4 wk. Mice were male and 14–16 wk old at the start of calorie restriction. (B) Lean mass measurements in AL and CR mice. (C) Stomach tissue from Lgr5-GFP reporter mouse showing endogenous fluorescence in AL and CR tissue. White box outlines high magnification region. Only antrum tissue is shown as gastric Lgr5+ cells in corpus demarcate a subpopulation of chief cells (Leushacke et al., 2017). (D) Quantification of Lgr5-GFP+ cells in Lgr5-GFP mice shown in C. (E) Quantification of Sox2+ cells in stomach tissue from FOXO1-Venus reporter mouse after CR. Metabolic data for these mice are shown in Fig. S1. (F) Immunohistochemistry (left) with quantification (right) of primary stomach cultures (PSC) generated from Lgr5-GFP mice stained for GFP. PSC were grown in control or serum-deprived (SD; 0.1% BSA) media and treated overnight with vehicle (DMSO) or γ -secretase inhibitor DAPT (10 μ M). (G and H) Immunohistochemistry of antral stomach tissue from AL and CR Lgr5-GFP reporter mice stained for Notch transcription factor Hes1 (G) and Notch ligand Jag1 (H). White scale bar is 100 μ m, yellow scale bar is 50 μ m. White arrow denotes Lgr5-GFP+ cell. DAPI counterstains nuclei. For each cell marker, percentage positive cells represent the number of immunoreactive+ cells (including Lgr5-GFP+ cells as indicated)/DAPI+ nuclei per microscope field. Bar graphs show mean \pm standard deviation. Each dot represents an individual mouse measurement (A and B) or quantification of a microscopic field from PSC (F) or AL (Lgr5-GFP mice: $n = 3$) and CR (Lgr5-GFP mice: $n = 3$) mice (D and E). * $P < 0.05$, ** $P < 0.01$, *** $P < 0.001$.

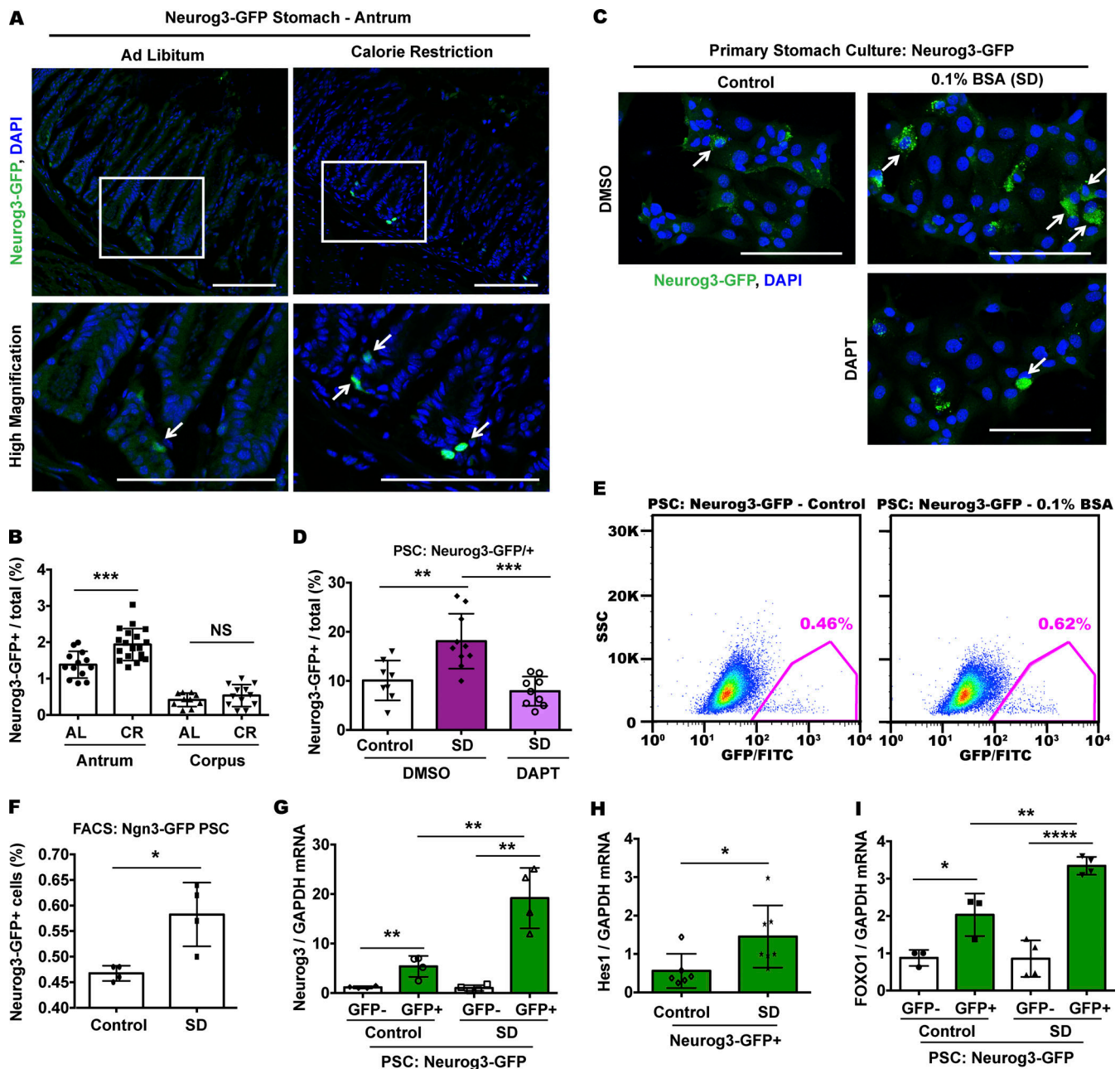


Figure 4. The abundance of endocrine progenitor cells is increased by calorie restriction through altered notch signaling. (A) Stomach tissue from Neurog3-GFP/+ reporter mice fed ad libitum (AL) or 30% food restricted (CR) for 4 wk. Mice were male and 14–16 wk old at the start of calorie restriction. Metabolic data for this cohort is displayed in Fig. 3, A and B. Endogenous GFP fluorescence is shown. White box outlines high magnification region. (B) Quantification of GFP+ cells in Neurog3-GFP/+ mice shown in A. (C and D) Representative images (C) with quantification (D) of primary stomach cultures (PSC) generated from Neurog3-GFP mice, cultured in control or serum-deprived (SD; 0.1% BSA) media, treated overnight with vehicle (DMSO) or γ -secretase inhibitor DAPT (10 μ M), and immunostained for GFP. (E) Representative FACS dot plots of primary stomach cells isolated from Neurog3-GFP/+ mice after overnight culture in control or SD media. GFP+ population is outlined in pink. (F) Quantification of GFP+ populations shown in E. Each dot is an independent preparation. (G–I) Gene expression in GFP– and GFP+ cell populations purified by FACS shown in panel E. PSC analyzed were from Neurog3-GFP mice after overnight culture in control or SD media. mRNA normalized to GAPDH. White scale bar is 100 μ m. White arrow denotes Neurog3-GFP+ cell. DAPI counterstains nuclei. For immunostaining, percentage positive cells represent the number of immunoreactive Neurog3-GFP+/DAPI+ nuclei per microscope field. For FACS, percentage GFP+ cells represents number of gated cells divided by total parent population. Bar graphs show mean \pm standard deviation. Each dot represents independent preparation of Neurog3-GFP PSC (F–I) or quantification of a microscopic field from PSC (D) or AL (Neurog3-GFP mice: $n = 4$) and CR (Neurog3-GFP mice: $n = 4$) mice (B). * $P < 0.05$, ** $P < 0.01$, *** $P < 0.001$, **** $P < 0.0001$. NS is not significant.

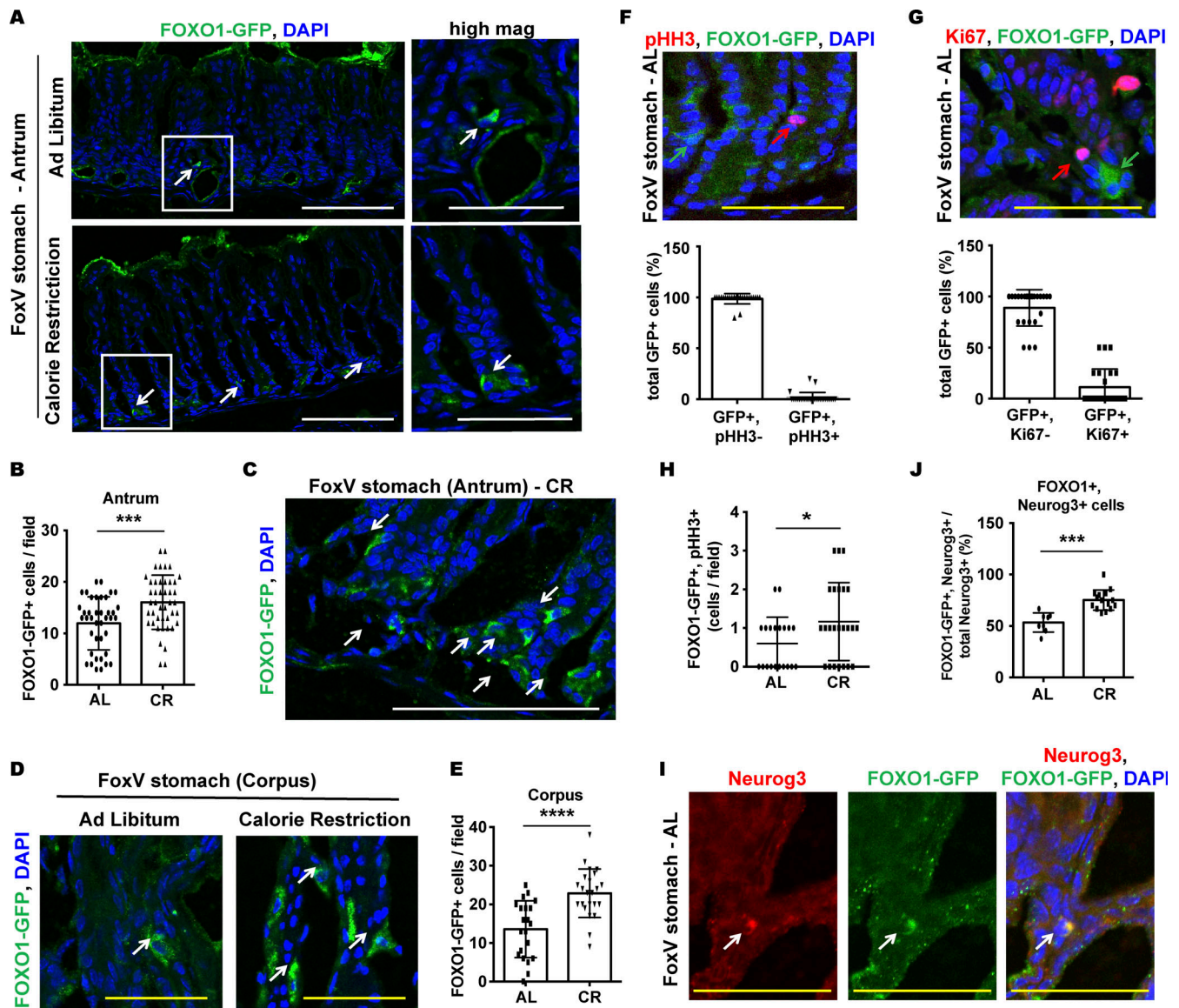


Figure 5. There are more gastric FOXO1+, Neuro3+ cells after calorie restriction. (A–C) Representative images (A, C) with quantification (panel B) of GFP staining (FOXO1-GFP; which recognizes FOXO1-Venus (FoxV) reporter) in the antrum of female FoxV mice after 4 wk of calorie restriction (CR, $n = 5$ mice) or in control mice fed ad libitum (AL, $n = 3$ mice). Mice were 12 wk old at the start of calorie restriction. Metabolic data for these mice are displayed in Fig. S1. White box outlines high magnification region. (D and E) Representative images (D) with quantification (E) of FOXO1-GFP staining in the corpus of AL and CR FoxV mice. (F and G) Immunostaining (top) with quantification (bottom) of FOXO1-GFP colocalization with proliferation markers phosphorylated histone H3 (pHH3; F) and Ki67 (G) in the stomach of AL FoxV mice. (H) In a separate experiment, quantification of FOXO1-GFP colocalization with pHH3 in stomach of female AL and CR FoxV mice. (I and J) Representative image (I) with quantification (J) of FOXO1-GFP and Neurogenin3 (Neuro3) colocalization in FoxV AL and CR mice. White and green arrows denote examples of FOXO1-GFP+ cells. Red arrow denotes pHH3+ and Ki67+ cell. White scale bar is 100 μm , yellow scale bar is 50 μm . DAPI counterstains nuclei. Bar graphs show mean \pm standard deviation. Each dot represents a quantification of a microscopic field from AL and CR mice (B, E, F–H, and J). * $P < 0.05$, *** $P < 0.001$, **** $P < 0.0001$.

male (Fig. 7 B) mice were food-restricted. To determine whether increased ghrelin contributed to the beneficial effects of calorie restriction, we blocked ghrelin signaling using the ghrelin receptor antagonist GHRP-6 (Asakawa et al., 2003) for 5 days. Importantly, we continued to calorie-restrict mice during this treatment, and both vehicle- and GHRP-6-treated mice consumed their food in its entirety throughout the duration of the experiment. While body weight was minimally increased in mice treated with GHRP-6 (Fig. 7 C), these mice had elevated fed glucose levels (GHRP-6: 144.2 ± 5.8 mg/dl versus Vehicle: $113.2 \pm$

5.3 mg/dl) (Fig. 7 D). In addition, the lean mass of GHRP-6-treated mice was similar to their lean mass prior to treatment, whereas vehicle-treated mice continued to lose lean mass due to continued food restriction (Fig. 7 E).

To test the involvement of Notch signaling, we next treated food-restricted mice with the Notch inhibitor PF-03084014 (PF), which blocks γ -secretase. While the 5-day treatment with PF did not alter body weight (Fig. 7 F), mice that received the Notch inhibitor had higher fed glucose levels compared with vehicle-treated controls (Fig. 7 G). Importantly, both groups consumed

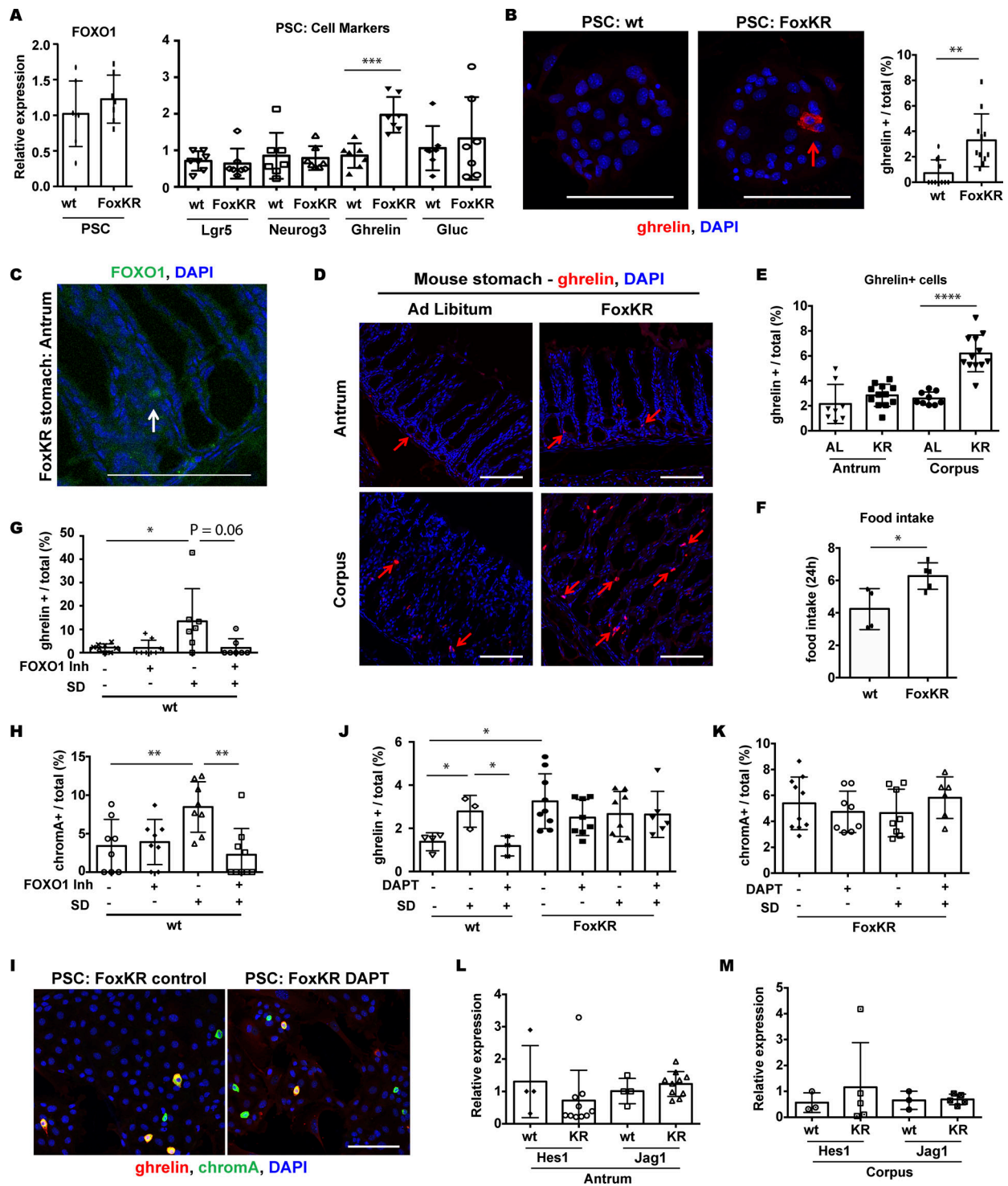


Figure 6. Nuclear FOXO1 promotes differentiation of ghrelin cells in primary stomach culture and in mice. (A) Gene expression in primary stomach cultures (PSC). Primary stomach cells were isolated from wild-type (wt) mice and mice homozygous for a constitutively active FOXO1 mutant (FoxKR) that localizes to the nucleus. Stomach markers include: *neurogenin3* (*Neurog3*) and *glucagon* (*Gluc*). Normalized to *E-cadherin* mRNA. (B) Representative image (left) with quantification (right) of PSC from indicated mice stained for Ghrelin. (C) Florescent staining for FOXO1 in FoxKR stomach. (D and E) Representative images (D) with quantification (E) of ghrelin+ cells in 12-wk-old female control (AL) and FoxKR (KR) stomach. AL ($n = 3$ mice) bars represent the same values quantified in Fig. 1D and KR ($n = 4$ mice). (F) Daily food intake measurements for female wild type (wt) ($n = 4$) and KR ($n = 5$) mice. Values presented represent an average 24 h intake measured over two consecutive days. (G and H) Quantification of ghrelin+ (G) and chromogranin A+ (ChromA, H) cells in wt PSC cultured under normal or serum-deprived (SD, 0.1% BSA) conditions and treated overnight with vehicle or 10 μ M FOXO1 inhibitor (Langlet et al., 2017) as indicated. (I) Immunofluorescence of FoxKR PSC cultured in normal media after overnight treatment with vehicle (control) or γ -secretase inhibitor DAPT (10 μ M). (J) Quantification of ghrelin+ cells in PSC from wt and KR mice grown in normal or SD media and treated overnight with DAPT. (K) Quantification of chromogranin A+ cells in FoxKR PSC at the indicated conditions. (L and M) Gene expression in the indicated wt and KR stomach tissue. Normalized to *GAPDH*

mRNA. Scale bar is 100 μ m. DAPI counterstains nuclei. Percentage positive cells represent the number of immunoreactive+ cells/DAPI+ nuclei per microscope field. Bar graphs show mean \pm standard deviation. Each dot represents an individual mouse measurement (F), quantification of a microscopic field from PSC (B, G, H, J, and K) or mice (E), or independent sample from mouse tissue (L and M) or PSC (A). * $P < 0.05$, ** $P < 0.01$, *** $P < 0.001$, and **** $P < 0.0001$.

all the food provided, which continued to be restricted for the duration of the experiment. Mice treated with PF also had minimal change in lean body mass, whereas animals receiving the vehicle had a significant decrease in lean mass after 5 days, consistent with calorie restriction (Fig. 7 H).

GIP and GLP-1 receptor agonists are being used to treat obesity and diabetes (Tan et al., 2022) and result in decreased eating. Daily treatment of wild-type mice with the dual- GIP/GLP1 receptor agonist tirzepatide (TZP) for 5 days significantly decreased weight (Fig. 7 I). TZP-treated mice had decreased food intake at the start of treatment, followed by normalization by treatment day 4 (Fig. 7 J). While mice had similar fed glucose levels at the start of the experiment, those receiving TZP had >50 mg/dl lower values (control: 142.6 ± 5.9 mg/dl versus TZP: 89.0 ± 2.6 mg/dl) by treatment day 5 (Fig. 7 K).

At the end of the experiment, TZP-treated mice also had decreased 5-h-fasting glucose (control: 138.8 ± 6.9 mg/dl versus TZP: 59.8 ± 5.9 mg/dl) (Fig. 7 L). Surprisingly, similar to calorie restriction, mice injected with TZP had an ~ 4.4 -fold increase in plasma ghrelin compared with vehicle (Fig. 7 M). This corresponded with an increased abundance of ghrelin+ cells in the antrum (control: $0.89\% \pm 0.20\%$ versus TZP: $2.26\% \pm 0.24\%$) and corpus (control: $1.44\% \pm 0.08\%$ versus TZP: $4.01\% \pm 0.38\%$) (Fig. 7 N and Fig. S5). Chromogranin A+ cells also increased by $\sim 400\%$ in the antrum and by $\sim 290\%$ in the corpus with TZP treatment (Fig. 7 O and Fig. S5). Taken together, these data suggest that ghrelin plays a role in the effects of TZP.

Discussion

We found that, unlike in the intestine, calorie restriction increased differentiated endocrine and Neurog3+ endocrine progenitor cells through increased Notch signaling in gastric Neurog3+ cells. We further show, using an active FOXO1 mutant, that FOXO1 localizes to the nucleus of Neurog3+ cells with calorie restriction, associated with an increased number of ghrelin cells.

Mechanistically, our data suggest that the increase in ghrelin+ cell number is dependent upon active FOXO1. FOXO1 regulates cellular differentiation and growth (Tsuchiya and Ogawa, 2017) and has been found in Neurog3+ and 5HT+ cells in the large and small intestines of mice and humans (Bouchi et al., 2014; Talchai et al., 2012). We have recently characterized a population of FOXO1+ cells in the stomach (McKimpson et al., 2022) that colocalize with markers of acid-secreting parietal as well as Neurog3+ cells. In these cells, FOXO1 regulates transcription of the cyclin E1 gene (CCNE1). Our data suggest that, under calorie restriction, FOXO1 marks an expanding subpopulation of Neurog3+ cells. Interestingly, FOXO1 is found in the nucleus of these cells and is associated with increased numbers of ghrelin cells. Evidence suggests that FOXO1 mediates changes occurring with calorie restriction in other tissues as well. For

example, FOXO1 haploinsufficiency is linked to reduced incidence of tumors with aging, although there was no effect on lifespan (Yamaza et al., 2010). FOXO1 also has been shown to have a role in maintaining telomere size during calorie restriction in the heart (Makino et al., 2016).

Here, we demonstrate that calorie restriction alters the abundance of stomach epithelial Neurog3+ cells by increasing Notch signaling. In support of Notch being activated in Neurog3+ cells, we found increased *Hes1* mRNA after serum deprivation. It remains to be determined what triggers Notch activation. Stem and progenitor cells in different tissues are sensitive to diet. For example, fasting promotes the function of Lgr5+ stem cells in the intestine by inducing fatty acid oxidation (Mihaylova et al., 2018). Prolonged fasting also promotes self-renewal of hematopoietic stem cells (Cheng et al., 2014). Conversely, mice fed a high-fat diet have increased numbers of intestinal stem cells through peroxisome proliferator-activated receptor delta (Beyaz et al., 2016). Interestingly, a low-lipid diet activates Notch signaling to influence cell differentiation in the *Drosophila* intestine (Obniski et al., 2018).

Notch regulates stomach Lgr5+ cell proliferation (Demitrack et al., 2015) through a DLL1-expressing niche cell located in the antral gland base to blunt their differentiation (Horita et al., 2022). Notch inhibition generally promotes differentiation. It is unclear why the opposite result is seen in the stomach after calorie restriction, but it may indicate a differential effect of Notch activation on proliferation and differentiation within specific stem and progenitor cell subpopulations, including Neurog3+ progenitor and Lgr5+ stem cells. In support of this, while Lgr5+ stem cells were decreased with calorie restriction, we saw increased Sox2+ cells, a distinct multipotent stem cell population in the stomach (Arnold et al., 2011). A different program may also be activated in gastric stem cells under calorie restriction compared with a normal diet. Notch-regulated Lgr5 stem cell maintenance is associated with increased mTOR signaling (Demitrack et al., 2015). While we did not assess mTOR signaling, calorie restriction modulates the function of intestinal stem cells through mTORC1 in Paneth cells, a component of the intestinal stem cell niche (Yilmaz et al., 2012). This expansion is dependent on mTORC1 and SIRT1 (Igarashi and Guarente, 2016). In mouse intestine, calorie restriction also preserves the function of a stem cells reserve pool by inhibiting mTORC1 (Yousefi et al., 2018).

Finally, our data demonstrate that ghrelin cell numbers increase upon calorie restriction. While we do not know whether ghrelin is secreted from these cells, this is likely in view of the increase in plasma ghrelin during fasting (Asakawa et al., 2001; Tschöp et al., 2000), confirmed in our experiments. A link between increased ghrelin and calorie restriction has been suggested (Reimer et al., 2010). Interestingly, ghrelin may also have a protective effect against aging (Cheng et al., 2010; Kaplan et al., 2017). It is not clear whether the increase in ghrelin+ cells is an

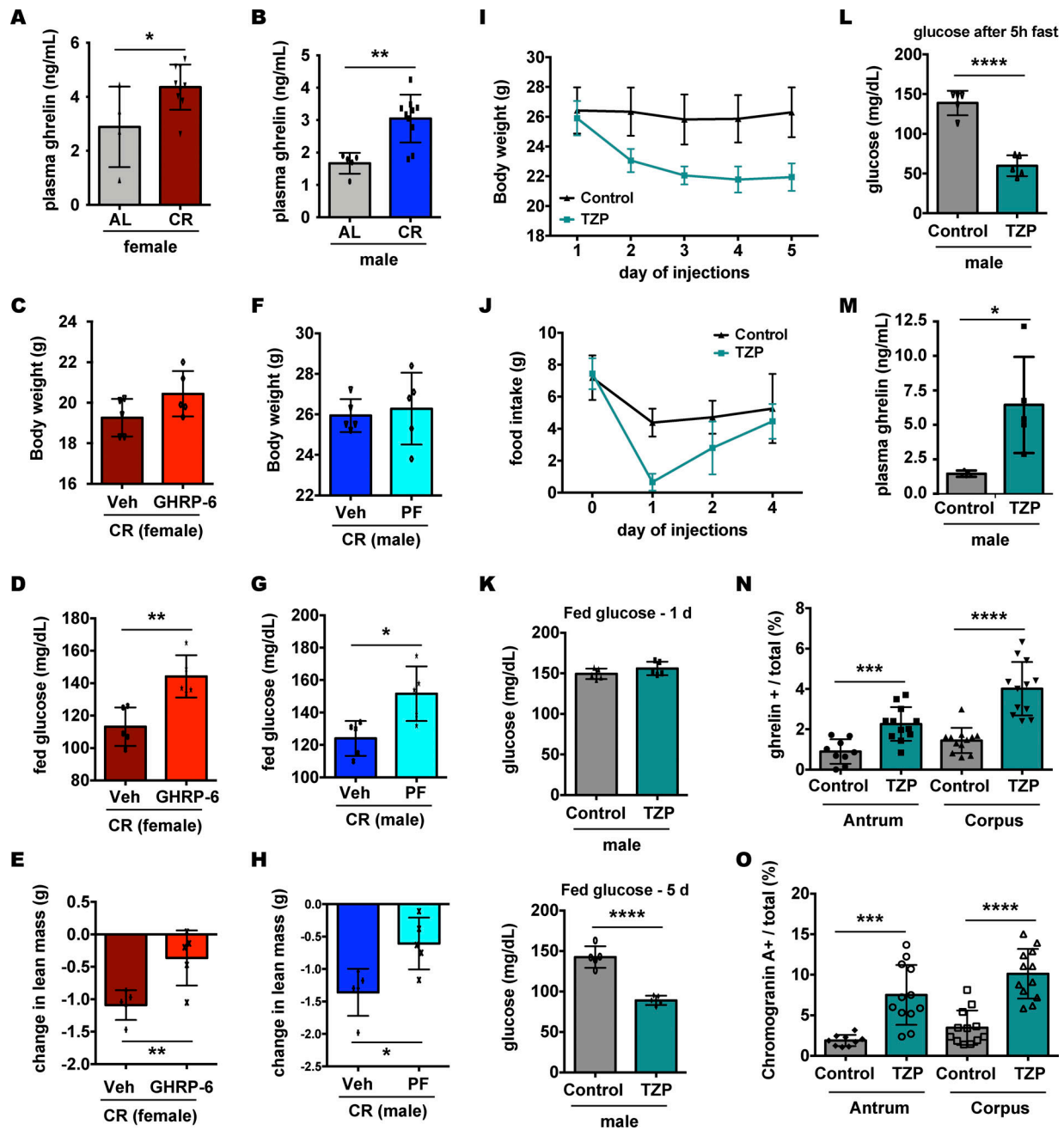


Figure 7. **Manipulating notch and ghrelin signaling in mice alters metabolism.** (A and B) Plasma ghrelin levels in female (A) and male (B) mice fed ad libitum (AL; female: $n = 4$, male: $n = 5$) or 30% food restricted (CR; female: $n = 10$, male: $n = 10$) for 4 wk. Mice were 14 wk of age at the start of calorie restriction. Metabolic data for these female and male cohorts are displayed in Fig. 1. (C–E) Body weight (C), fed glucose (D), and change in lean mass during treatment (E) in female CR mice (30% food restriction for 4 wk) subsequently treated daily with Vehicle (Veh) or ghrelin receptor antagonist [D-Lys-3]-GHRP-6 (GHRP-6) for 5 days at the concentration 200 nmol/mouse. (F–H) Body weight (F), fed glucose (G), and change in lean mass during treatment (H) in male CR mice (30% food restriction for 4 wk) subsequently injected daily with Veh or 150 mg/kg of the Notch inhibitor PF-03084014 (PF) for 5 days. Data in I through O is from male wild-type mice (13 wk old) that were treated daily with vehicle (Control; $n = 5$ mice) or 30 nM/kg tirzepatide (TZP; $n = 5$ mice) for 5 days. (I) Daily body weight measurements. (J) Consecutive food intake. (K) Fed glucose after 1 and 5 day TZP treatment. (L) Blood glucose measurements after a 5 h fast after 5 days TZP treatment. (M) Plasma ghrelin measurements after 5 days TZP treatment. (N and O) Quantification of ghrelin+ (N) and chromogranin A+ (O) cells in the stomach tissue of mice after TZP treatment. Representative fluorescent images are displayed in Fig. S5. Percentage positive cells represent the number of immunoreactive+ cells/DAPI+ nuclei per microscope field. Bar graphs show mean \pm standard deviation. Each dot is an individual mouse (A–H, and K–M) or microscope field (panels N and O). * $P < 0.05$, ** $P < 0.01$, *** $P < 0.001$, **** $P < 0.0001$.

adaptive change to decreased food consumption or a protective effect of calorie restriction itself. Our *in vivo* data suggested the contribution of the latter, as blocking this pathway in food-restricted mice with either a Notch inhibitor or ghrelin receptor antagonist elevates glucose levels without affecting food intake. This pathway may also be broadly activated, as treatment of mice with the weight loss agent tirzepatide (Tan et al., 2022) also triggers the expansion of stomach ghrelin-producing cells, although a contributing factor may be the minimal food intake in TZP-treated mice, particularly within the first 2 days of treatment.

Taken together, our data suggest that the expansion of Neurog3+ endocrine cells into lineage-committed ghrelin-producing cells during calorie restriction contributes to the beneficial protective effects of calorie restriction, including improved metabolism.

Materials and methods

Animal studies

FoxV mice were generated as previously described (Kuo et al., 2019). Neurog3-GFP (Lee et al., 2002) and FoxKR (Banks et al., 2011) mice were previously described, and Lgr5-GFP (strain #008875; RRID:IMSR_JAX:008875), NICD (strain #008159; RRID:IMSR_JAX:008159), and Tomato (strain #007909; RRID:IMSR_JAX:007909) mice were purchased from Jackson Laboratories. All mice were maintained on C57BL/6J background. Unless it is otherwise indicated, tissue and primary stomach cells were from mice 10–12 wk of age. Calorie restriction was performed in mice 12–16 wk old at the start of food restriction. Thus, tissue for these experiments, collected upon the completion of food restriction, was collected from mice that were 16–20 wk age. The specific age and biological sex of each cohort are indicated in each figure legend. Male and female mice were used in equal numbers and as indicated in the figure legends. All studies were approved by the Columbia University Institutional Animal Care and Utilization Committee.

Calorie restriction

Mice were fed a standard chow diet (SCD) (13.1, 62.4, and 24.5% calories from fat, carbohydrate, and protein respectively; Pico-Lab Rodent Diet 20, 5053; Purina Mills). All mice were acclimated to being singly housed for a week with individual food intake determined over the last 3 days. Thereafter, mice were assigned to groups with an equal starting body mass and either had access to food and water *ad libitum* (AL) or were calorie-restricted (CR) by 30% with food placed into the cage twice daily for 4 wk. CR mice received 2.6–2.8 g/day of SCD per mouse. Plasma ghrelin was measured using a Rat/Mouse Ghrelin (Total) ELISA kit (Millipore Sigma) where samples were assessed in blood collected from AL and CR mice after 5 h fast (food removed at 9 am and blood collected at 2 pm). Blood glucose was measured under fed conditions or after 5 h fast using a OneTouch glucose monitoring system (LifeScan). Lean mass was measured by EchoMRI. For tissue collection, to mimic *ad libitum* conditions, CR mice were given their last feeding at 9 am and tissue collected ~3 h later at noon.

Drug treatments

Notch activity in mice was blocked using PF-03084014 (PF) (Nirogacestat from SelleckChem) (Kitamoto et al., 2022). Specifically, PF was resuspended in N,N-Dimethylacetamide:Kolliphor HS 15: water = 5:10:85 (vol/vol/vol) solution, pH 4~5, to a working concentration of 15 mg/ml using sonication. Mice were injected IP daily (at ~4 pm) with vehicle or PF at the final dose of 150 mg/kg for 5 days. Ghrelin activity was blocked using the ghrelin receptor antagonist [D-Lys-3]-GHRP-6 (GHRP-6) (Bachem) (Asakawa et al., 2003). Specifically, GHRP-6 was resuspended in saline and administered by intraperitoneal (IP) injection for 5 days at the concentration 200 nmol/mouse. Prior to PF and GHRP-6 treatments, mice were calorie-restricted by 30% for 4 wk. Mice were 14 wk old at the start of caloric restriction and food restriction was continued throughout the duration of the treatments. Male mice were used for PF treatments and female mice were used for GHRP-6 treatments. Tirzepatide (MedChemExpress) was resuspended in dimethyl sulfoxide at a stock concentration of 1 mM. The drug was further diluted 1:100 with 1xPBS to create a working solution. 13-wk-old male mice were injected IP with either vehicle (1xPBS) or TZP at a concentration of 30 nM/kg daily (at ~4 pm) for 5 days. The following day, mice were fasted at 9 am for 5 h, blood glucose was measured and collected (to measure ghrelin levels), and the tissue was collected for analysis. Throughout the duration of the experiment, mice were measured for food intake, body weight, and fed glucose levels.

Fluorescent imaging

After dissection, the stomach tissue was fixed in 4% paraformaldehyde (PFA, cat no. 15710; Electron Microscopy Sciences) for 1.5 h on ice. Tissue was subsequently placed in 30% sucrose (in 1xPBS) overnight, embedded in OCT, flash frozen, and sectioned at 5 μ m for staining. For primary cultures, cells were grown on gelatin-coated chamber slides (cat. no. 354114; Corning), fixed in 4% paraformaldehyde for 10 m at room temperature, and permeabilized in PBS with 0.1% Triton X-100 (Cat. no. 42235-5000; Acros Organics) for 10 min.

For immunohistochemistry, tissue was blocked in 10% goat (Cat. no. S-1000; Vector) or donkey (cat. no. 017000121; Jackson Immuno Research Labs) serum for 1 h at room temperature and then incubated with primary antibodies diluted in blocking solution overnight. The primary antibodies used were as follows: GFP (cat no. A-6455, 1:200; RRID:AB_221570; Molecular Probes), GFP (cat no. ab6662, 1:100; RRID:AB_305635; Abcam), Ghrelin (cat no. MAB8200, 1:100; RRID:AB_2637039; Novus Biologicals), Ki67 (cat no. ab16667, 1:50; RRID:AB_302459; Abcam), Neurogenin3 (cat no. ab38548, 1:50; RRID:AB_776709; Abcam), Sox2 (cat no. ab97959, 1:200; RRID:AB_2341193; Abcam), Chromogranin A (cat no. ab45179, 1:200; RRID:AB_726879; Abcam), 5HT (cat. no. NB120-16007, 1:50; RRID:AB_792022; Novus Biologicals), Gastrin (cat no. ab232775, 1:200, RRID:AB_3097695; Abcam), Glucagon (cat no. M182, 1:500; RRID:AB_2619627; Takara), CCK (cat no. PA5-32348, 1:400; RRID:AB_2549819; Thermo Fisher Scientific), Synaptophysin (cat no. MAB5258, 1:200; RRID:AB_2313839; Millipore), Jag1 (cat no. AF599, 1:100; RRID:AB_2128257; R and D), Hes1 (cat no. sc25392, 1:100; RRID:

AB_647996; Santa Cruz), and pHH3 (cat no. ab5176, 1:100; RRID: AB_304763; Abcam). Alexa Fluor 488, 568, and 647 (dil. 1:1,000; Molecular Probes) secondary antibodies of corresponding species were used to detect primary antibodies. All secondaries were diluted 1:1,000 in blocking serum and incubated for 1 h at room temperature. Coverslips were applied using VECTA-SHIELD Vibrance Antifade Mounting Medium with DAPI (cat no. H-1800-10; Vector Laboratories) to counterstain nuclei. Images were obtained at room temperature using a Zeiss LSM 710 confocal microscope (Zeiss) and a Plan-Apochromat objective (20 ×/0.8) using ZEN (black edition) software. Images were taken in black and white and pseudocolored as indicated in the figures. When needed to optimize visualization, minor adjustments to brightness and contrast were performed to the entire image equally using ZEN (black edition) software. No additional imaging processing was performed.

Primary stomach culture

Primary stomach cells were isolated from the indicated mice (McKimpson et al., 2022). Specifically, after serosa was removed, the antral stomach was incubated with digestion buffer (5 mM EDTA [cat. no. 15575-038; Invitrogen] in 1xPBS) at 4°C for 1.5 h. Following second digestion at 37°C for 30 m in TrypLE (cat. no. 12604013; Invitrogen) supplemented with 2 U/μl DNase-1 (cat. no. 10104159001; Sigma-Aldrich) and 10 μM Y-27632 (cat. no. Y0503-1 MG; Rock Inhibitor, Sigma-Aldrich), cells were washed in ice-cold basic media (Advanced DMEM/F12 [cat. no. 12634010; Invitrogen] supplemented with 10 mM HEPES [cat. no. 15630080; Invitrogen], 1 x Glutamax [cat. no. 35050061; Invitrogen], 1% pen/strep [cat. no. 15140-122; Gibco], and 1% bovine serum albumin, fraction V [cat. no. BP1600-100; Thermo Fisher Scientific]) and passed through a 40-μM cell strainer (cat. no. 22363547; Thermo Fisher Scientific).

For 2-D culture, primary stomach cells were plated on mouse embryonic fibroblasts (cat. no. A34180; Gibco) at density 5×10^6 cells/six-well plate coated with gelatin (cat. no. ES-006-B; Millipore). Cells were cultured in basic culture media (described above) supplemented with 10 μM rock inhibitor, 1 x N2 supplement (cat. no. 17502048; Invitrogen), 1 x B-27 supplement (cat. no. 17504044; Invitrogen), 1 mM N-Acetyl-L-cysteine (cat. no. A9165-5 G; Sigma-Aldrich), and 1 x Primocin (cat. no. NC9141851; Invitrogen). Rock inhibitor was removed from media after overnight recovery. Media for serum-deprivation conditions was modified to contain 0.1% bovine serum albumin, fraction V. Cells were cultured overnight at serum-deprived conditions. Where indicated, cells were treated overnight with 10 μM DAPT (N-[N-(3, 5-difluorophenacetyl)-l-alanyl]-s-phenylglycine-butyl ester), 4 μM TAT-cre (cat. no. SCR508; Millipore), or 10 μM FOXO1 inhibitor (AstroZeneca; Compound 10 as published in Langlet et al., [2017]).

FACS

After culture, primary stomach cells were collected using trypsin and resuspended in basic culture media. Prior to sorting, cells were stained with the impermeant DNA dye DAPI. Cells were sorted using a BD Influx with a blue (488-nm) laser and 530/40 bandpass filter to detect endogenous GFP fluorescence

and a green (561-nm) laser and 610/20 bandpass filter to detect tomato fluorescence and analyzed using FlowJo software (BD Life Sciences). To determine single-cell populations, cells were gated based on forward and side scatter and trigger pulse width. In addition, only viable cells (negative for DAPI) were considered for downstream analysis of GFP fluorescence.

qPCR

RNA was isolated from primary stomach cultures using an Arcturus PicoPure RNA Isolation Kit (cat no. KIT0204; Applied Biosystems) as recommended by the manufacturer with the addition of the optional 15-minute DNaseI treatment. cDNA was generated from RNA using qScript cDNA SuperMix (cat no. 101414-106; Quanta Biosciences) by diluting RNA with 5x master mix, without adding any additional water, and incubating samples at 25°C for 5 m, 42°C for 30 m, 85°C for 5 m, and holding at 4°C (McKimpson and Accili, 2019). qPCR reactions were completed using GoTaq qPCR Master Mix (Promega) with the following primer pairs: *Hes1*: forward: 5'-CACTGATTTGGATG CACTTAAGAAG-3', reverse: 5'-CCGGGGTAGTTCATGGCGTTG ATCT-3'; *Jagl1*: forward: 5'-CCTCGGGTCAGTTTGAGCTG-3', reverse: 5'-CCTTGAGGCACACTTTGAAGTA-3'; *Foxo1*: forward: 5'-TCCAGTTCCTTCATTCTGCACT-3', reverse: 5'-GCGTGCCCTACT TCAAGGATAA-3'; *E-cadherin*: forward: 5'-AGCTTTTCCGCGCTC CTG-3', reverse: 5'-CTTCCGAAAAGAAGGCTGTCC-3'; *Ghrelin*: forward: 5'-GCCAGCAGAGAAAGGAATCCA-3', reverse: 5'-GCG CCTCTTTGACCTCTTCC-3'; *Glucagon*: forward: 5'-ATGAAGACC ATTTACTTTGTGGCTG-3', reverse: 5'-CGGCCTTTCACCAGCCAC GC-3'; *Chromogranin A*: forward: 5'-CAGTCGTCCACTCTTTCCG-3', reverse: 5'-CCTCTCGTCTCCTTGGAGGG-3'; *GAPDH*: forward: 5'-CGT ATTGGGGCCTGGTAC-3', reverse: 5'-ATGATGACCCCTTTGGCTCC-3'; *Lgr5*: forward: 5'-ACCCGCCAGTCTCTACATC-3', reverse: 5'-GCA TCTAGGCGCAGGGATTG-3'; and *Ngn3*: forward: 5'-TGGCCCATAGAT GATGTTCC-3', reverse: 5'-AGAAGGCAGATCACCTTCGTG-3'. Using a Bio-Rad CFX96 real-time PCR system for measurements, relative gene expression was calculated using the $\Delta\Delta C_t$ method with *E-cadherin* (as an epithelial marker of stomach cells) as the reference gene for primary stomach cultures and with *GAPDH* as the reference gene for sorted cells.

Quantification

For the quantification of tissue, at least at least five independent fields/samples for a minimum of three mice in each experimental group were quantified. No samples were excluded from the analysis. Unless otherwise indicated, each dot in graphs of quantification of microscopic images represents an independent field. For each field, the percentage of positive cells was calculated for each marker by dividing the total immunoreactive+ cell by the total epithelial DAPI+ nuclei in the same field. For each sample, quantification was performed separately for antrum and corpus stomach. Note that *Lgr5*-GFP+ cells were only assessed in antrum to avoid any confounding effects from *Lgr5*-expressing chief cells in the corpus (Leushacke et al., 2017). To assess the proliferation of GFP+ cells in FoxV reporter mice, each FOXO1-GFP+ cell was determined to be positive or negative for respective proliferation markers, and the prevalence of each was assessed as a ratio over total GFP+ cell number for each

microscopic field. The number of specific mice for each experiment is indicated in figure legends. For primary cultures, stomach cells in six to eight microscopic fields for at least three independent cultures were quantified.

Statistics

A two-tailed student's *t* test was used to compare the two groups. Analysis of variance followed by a Tukey post-hoc test was used to compare multiple groups. Data distribution was assumed to be normal, but this was not formally tested. GraphPad Prism 6 software was used for calculations and $P < 0.05$ was considered significant. Graphs are depicted as average \pm standard deviation with individual samples being indicated using individual points. The specific measurements of each sample (i.e., mouse measurements and quantification of microscopic field) are as indicated in each of the figure legends.

Online supplemental material

This article contains five supplemental figures. **Fig. S1** shows body weight, lean mass, and fasting glucose measurements from female mice before and after 4 wk of calorie restriction. **Fig. S2** provides representative low-magnification fluorescent images of gastric endocrine cells in tissue from female mice fed ad libitum or calorie-restricted. **Fig. S3** shows representative low-magnification fluorescent images showing the abundance of ghrelin+ and chromogranin A+ cells in the stomach tissue of male ad libitum-fed and calorie-restricted mice. **Fig. S4** presents control staining for FOXO1-GFP for interpretation of results from FOXO1-Venus reporter mice. **Fig. S5** shows representative fluorescent images of ghrelin+ and chromogranin A+ cells in stomach tissue from male mice treated with tirzepatide (TZP).

Data availability

Data are available in the article itself and its supplementary materials. The data are available from the corresponding author upon reasonable request.

Acknowledgments

We thank members of the Accili laboratory for insightful discussions and Tommy Kolar, Ana M. Flete-Castro, Xi Sun, and Lu Caisheng for technical support.

This research was supported by a Naomi Berrie Diabetes Center (Columbia University) Berrie Fellow in Diabetes Research Award and National Institute of Diabetes and Digestive and Kidney Diseases (NIDDK) grant nos. K01DK121873 to W.M. McKimpon., DK103818 to U. Pajvani, and DK57539 to D. Accili. These studies used the CCTI Flow Cytometry Core, supported by NIH Office of the Director grant no. S10OD020056, and the resources of the Diabetes Research Center Flow Core, supported by NIDDK grant no. P30DK063608. D. Accili was a founder, director, stockholder, and chair of the board of Forkhead Biotherapeutics Corp.

Author contributions: W.M. McKimpon: Conceptualization, Data curation, Formal analysis, Funding acquisition, Investigation, Methodology, Project administration, Resources, Supervision, Validation, Visualization, Writing—original draft, Writing

– review & editing, S. Spiegel: Formal analysis, Investigation, Visualization, M. Mukhanova: Investigation, Writing—review & editing, M. Kraakman: Investigation, W. Du: Investigation, Resources, T. Kitamoto: Investigation, Resources, Writing—review & editing, J. Yu: Resources, Z. Deng: Data curation, Methodology, Resources, U. Pajvani: Conceptualization, Funding acquisition, Supervision, Writing—review & editing, D. Accili: Conceptualization, Data curation, Formal analysis, Funding acquisition, Investigation, Methodology, Project administration, Resources, Supervision, Validation, Visualization, Writing—original draft, Writing—review & editing.

Disclosures: The authors declare no competing interests exist.

Submitted: 23 May 2023

Revised: 2 May 2024

Accepted: 20 June 2024

References

- Arnold, K., A. Sarkar, M.A. Yram, J.M. Polo, R. Bronson, S. Sengupta, M. Seandel, N. Geijsen, and K. Hochedlinger. 2011. Sox2(+) adult stem and progenitor cells are important for tissue regeneration and survival of mice. *Cell Stem Cell*. 9:317–329. <https://doi.org/10.1016/j.stem.2011.09.001>
- Asakawa, A., A. Inui, T. Kaga, G. Katsuura, M. Fujimiya, M.A. Fujino, and M. Kasuga. 2003. Antagonism of ghrelin receptor reduces food intake and body weight gain in mice. *Gut*. 52:947–952. <https://doi.org/10.1136/gut.52.7.947>
- Asakawa, A., A. Inui, T. Kaga, H. Yuzuriha, T. Nagata, N. Ueno, S. Makino, M. Fujimiya, A. Nijima, M.A. Fujino, and M. Kasuga. 2001. Ghrelin is an appetite-stimulatory signal from stomach with structural resemblance to motilin. *Gastroenterology*. 120:337–345. <https://doi.org/10.1053/gast.2001.22158>
- Baggio, L.L., and D.J. Drucker. 2007. Biology of incretins: GLP-1 and GIP. *Gastroenterology*. 132:2131–2157. <https://doi.org/10.1053/j.gastro.2007.03.054>
- Banks, A.S., J.Y. Kim-Muller, T.L. Mastracci, N.M. Kofler, L. Qiang, R.A. Haeusler, M.J. Jurczak, D. Laznik, G. Heinrich, V.T. Samuel, et al. 2011. Dissociation of the glucose and lipid regulatory functions of FoxO1 by targeted knockin of acetylation-defective alleles in mice. *Cell Metab.* 14: 587–597. <https://doi.org/10.1016/j.cmet.2011.09.012>
- Barker, N., M. Huch, P. Kujala, M. van de Wetering, H.J. Snippert, J.H. van Es, T. Sato, D.E. Stange, H. Begthel, M. van den Born, et al. 2010. Lgr5(+ve) stem cells drive self-renewal in the stomach and build long-lived gastric units in vitro. *Cell Stem Cell*. 6:25–36. <https://doi.org/10.1016/j.stem.2009.11.013>
- Barker, N., J.H. van Es, J. Kuipers, P. Kujala, M. van den Born, M. Cozijnsen, A. Haeghebarth, J. Korving, H. Begthel, P.J. Peters, and H. Clevers. 2007. Identification of stem cells in small intestine and colon by marker gene Lgr5. *Nature*. 449:1003–1007. <https://doi.org/10.1038/nature06196>
- Beyaz, S., M.D. Mana, J. Roper, D. Kedrin, A. Saadatpour, S.J. Hong, K.E. Bauer-Rowe, M.E. Xifaras, A. Akkad, E. Arias, et al. 2016. High-fat diet enhances stemness and tumorigenicity of intestinal progenitors. *Nature*. 531:53–58. <https://doi.org/10.1038/nature17173>
- Bouchi, R., K.S. Foo, H. Hua, K. Tsuchiya, Y. Ohmura, P.R. Sandoval, L.E. Ratner, D. Egli, R.L. Leibel, and D. Accili. 2014. FOXO1 inhibition yields functional insulin-producing cells in human gut organoid cultures. *Nat. Commun.* 5:4242. <https://doi.org/10.1038/ncomms5242>
- Cheng, C.W., G.B. Adams, L. Perin, M. Wei, X. Zhou, B.S. Lam, S. Da Sacco, M. Mirisola, D.I. Quinn, T.B. Dorff, et al. 2014. Prolonged fasting reduces IGF-1/PKA to promote hematopoietic-stem-cell-based regeneration and reverse immunosuppression. *Cell Stem Cell*. 14:810–823. <https://doi.org/10.1016/j.stem.2014.04.014>
- Cheng, K.C., Y.X. Li, A. Asakawa, and A. Inui. 2010. The role of ghrelin in energy homeostasis and its potential clinical relevance (Review). *Int. J. Mol. Med.* 26:771–778. <https://doi.org/10.3892/ijmm.00000524>
- Colman, R.J., R.M. Anderson, S.C. Johnson, E.K. Kastman, K.J. Kosmatka, T.M. Beasley, D.B. Allison, C. Cruzen, H.A. Simmons, J.W. Kemnitz, and R. Weindruch. 2009. Caloric restriction delays disease onset and mortality in rhesus monkeys. *Science*. 325:201–204. <https://doi.org/10.1126/science.1173635>

- Demitrack, E.S., G.B. Gifford, T.M. Keeley, A.J. Carulli, K.L. VanDussen, D. Thomas, T.J. Giordano, Z. Liu, R. Kopan, and L.C. Samuelson. 2015. Notch signaling regulates gastric antral LGR5 stem cell function. *EMBO J.* 34:2522–2536. <https://doi.org/10.15252/embj.201490583>
- Drucker, D.J. 2007. The role of gut hormones in glucose homeostasis. *J. Clin. Invest.* 117:24–32. <https://doi.org/10.1172/JCI30076>
- Forni, M.F., J. Peloggia, T.T. Braga, J.E.O. Chinchilla, J. Shinohara, C.A. Navas, N.O.S. Camara, and A.J. Kowaltowski. 2017. Caloric restriction promotes structural and metabolic changes in the skin. *Cell Rep.* 20:2678–2692. <https://doi.org/10.1016/j.celrep.2017.08.052>
- Gribble, F.M., and F. Reimann. 2016. Enteroendocrine cells: Chemosensors in the intestinal epithelium. *Annu. Rev. Physiol.* 78:277–299. <https://doi.org/10.1146/annurev-physiol-021115-105439>
- Horita, N., T.M. Keeley, E.S. Hibdon, E. Delgado, D. Lafkas, C.W. Siebel, and L.C. Samuelson. 2022. Delta-like 1-expressing cells at the gland base promote proliferation of gastric antral stem cells in mouse. *Cell. Mol. Gastroenterol. Hepatol.* 13:275–287. <https://doi.org/10.1016/j.jcmgh.2021.08.012>
- Igarashi, M., and L. Guarente. 2016. mTORC1 and SIRT1 cooperate to foster expansion of gut adult stem cells during calorie restriction. *Cell.* 166:436–450. <https://doi.org/10.1016/j.cell.2016.05.044>
- Il'yasova, D., L. Fontana, M. Bhopkar, C.F. Pieper, I. Spasojevic, L.M. Redman, S.K. Das, K.M. Huffman, W.E. Kraus, and CALERIE Study Investigators. 2018. Effects of 2 years of caloric restriction on oxidative status assessed by urinary F2-isoprostanes: The CALERIE 2 randomized clinical trial. *Aging Cell.* 17:e12719. <https://doi.org/10.1111/accel.12719>
- Kaplan, R.C., G. Strizich, C. Aneke-Nash, C. Dominguez-Islas, P. Bužková, H. Strickler, T. Rohan, M. Pollak, L. Kuller, J.R. Kizer, et al. 2017. Insulinlike growth factor binding protein-1 and ghrelin predict health outcomes among older adults: Cardiovascular health study cohort. *J. Clin. Endocrinol. Metab.* 102:267–278. <https://doi.org/10.1210/jc.2016-2779>
- Kitamoto, T., Y.K. Lee, N. Sultana, H. Watanabe, W.M. McKimpon, W. Du, J. Fan, B. Diaz, H.V. Lin, R.L. Leibel, et al. 2022. Chemical induction of gut β -like-cells by combined FoxO1/Notch inhibition as a glucose-lowering treatment for diabetes. *Mol. Metab.* 66:101624. <https://doi.org/10.1016/j.molmet.2022.101624>
- Kojima, M., H. Hosoda, Y. Date, M. Nakazato, H. Matsuo, and K. Kangawa. 1999. Ghrelin is a growth-hormone-releasing acylated peptide from stomach. *Nature.* 402:656–660. <https://doi.org/10.1038/45230>
- Kuo, T., M.J. Kraakman, M. Damle, R. Gill, M.A. Lazar, and D. Accili. 2019. Identification of C2CD4A as a human diabetes susceptibility gene with a role in β cell insulin secretion. *Proc. Natl. Acad. Sci. USA.* 116:20033–20042. <https://doi.org/10.1073/pnas.1904311116>
- Langlet, F., R.A. Haeusler, D. Lindén, E. Ericson, T. Norris, A. Johansson, J.R. Cook, K. Aizawa, L. Wang, C. Buettner, and D. Accili. 2017. Selective inhibition of FOXO1 activator/repressor balance modulates hepatic glucose handling. *Cell.* 171:824–835.e18. <https://doi.org/10.1016/j.cell.2017.09.045>
- Lee, C.S., N. Perreault, J.E. Brestelli, and K.H. Kaestner. 2002. Neurogenin 3 is essential for the proper specification of gastric enteroendocrine cells and the maintenance of gastric epithelial cell identity. *Genes Dev.* 16:1488–1497. <https://doi.org/10.1101/gad.985002>
- Leushacke, M., S.H. Tan, A. Wong, Y. Swathi, A. Hajamohideen, L.T. Tan, J. Gong, E. Wong, S.L.I.J. Deng, K. Murakami, and N. Barker. 2017. Lgr5-expressing chief cells drive epithelial regeneration and cancer in the oxyntic stomach. *Nat. Cell Biol.* 19:774–786. <https://doi.org/10.1038/ncb3541>
- Ma, S., S. Sun, L. Geng, M. Song, W. Wang, Y. Ye, Q. Ji, Z. Zou, S. Wang, X. He, et al. 2020. Caloric restriction reprograms the single-cell transcriptional landscape of *Rattus norvegicus* aging. *Cell.* 180:984–1001.e22. <https://doi.org/10.1016/j.cell.2020.02.008>
- Madeo, F., D. Carmona-Gutierrez, S.J. Hofer, and G. Kroemer. 2019. Caloric restriction mimetics against age-associated disease: Targets, mechanisms, and therapeutic potential. *Cell Metab.* 29:592–610. <https://doi.org/10.1016/j.cmet.2019.01.018>
- Makino, N., J. Oyama, T. Maeda, M. Koyanagi, Y. Higuchi, I. Shimokawa, N. Mori, and T. Furuyama. 2016. FoxO1 signaling plays a pivotal role in the cardiac telomere biology responses to calorie restriction. *Mol. Cell. Biochem.* 412:119–130. <https://doi.org/10.1007/s11010-015-2615-8>
- McCay, C.M., M.F. Crowell, and L.A. Maynard. 1989. The effect of retarded growth upon the length of life span and upon the ultimate body size. 1935. *Nutrition.* 5:155–171, discussion: 172.
- McKimpson, W.M., and D. Accili. 2019. A fluorescent reporter assay of differential gene expression response to insulin in hepatocytes. *Am. J. Physiol. Cell Physiol.* 317:C143–C151. <https://doi.org/10.1152/ajpcell.00504.2018>
- McKimpson, W.M., T. Kuo, T. Kitamoto, S. Higuchi, J.C. Mills, R.A. Haeusler, and D. Accili. 2022. FOXO1 is present in stomach epithelium and determines gastric cell distribution. *Gastro Hep Adv.* 1:733–745. <https://doi.org/10.1016/j.gastha.2022.05.005>
- Mihaylova, M.M., C.W. Cheng, A.Q. Cao, S. Tripathi, M.D. Mana, K.E. Bauer-Rowe, M. Abu-Remaleh, L. Clavain, A. Erdemir, C.A. Lewis, et al. 2018. Fasting activates fatty acid oxidation to enhance intestinal stem cell function during homeostasis and aging. *Cell Stem Cell.* 22:769–778.e4. <https://doi.org/10.1016/j.stem.2018.04.001>
- Most, J., L.A. Gilmore, S.R. Smith, H. Han, E. Ravussin, and L.M. Redman. 2018. Significant improvement in cardiometabolic health in healthy nonobese individuals during caloric restriction-induced weight loss and weight loss maintenance. *Am. J. Physiol. Endocrinol. Metab.* 314:E396–E405. <https://doi.org/10.1152/ajpendo.00261.2017>
- Obniski, R., M. Sieber, and A.C. Spradling. 2018. Dietary lipids modulate notch signaling and influence adult intestinal development and metabolism in *Drosophila*. *Dev. Cell.* 47:98–111.e5. <https://doi.org/10.1016/j.devcel.2018.08.013>
- Qiang, L., K. Tsuchiya, J.Y. Kim-Muller, H.V. Lin, C. Welch, and D. Accili. 2012. Increased atherosclerosis and endothelial dysfunction in mice bearing constitutively deacetylated alleles of Foxo1 gene. *J. Biol. Chem.* 287:13944–13951. <https://doi.org/10.1074/jbc.M111.332767>
- Ravussin, E., L.M. Redman, J. Rochon, S.K. Das, L. Fontana, W.E. Kraus, S. Romashkan, D.A. Williamson, S.N. Meydani, D.T. Villareal, et al. 2015. A 2-year randomized controlled trial of human caloric restriction: Feasibility and effects on predictors of health span and longevity. *J. Gerontol. A. Biol. Sci. Med. Sci.* 70:1097–1104. <https://doi.org/10.1093/geron/glv057>
- Redman, L.M., S.R. Smith, J.H. Burton, C.K. Martin, D. Il'yasova, and E. Ravussin. 2018. Metabolic slowing and reduced oxidative damage with sustained caloric restriction support the rate of living and oxidative damage theories of aging. *Cell Metab.* 27:805–815.e4. <https://doi.org/10.1016/j.cmet.2018.02.019>
- Reimer, R.A., A.D. Maurer, D.C. Lau, and R.N. Auer. 2010. Long-term dietary restriction influences plasma ghrelin and GOAT mRNA level in rats. *Physiol. Behav.* 99:605–610. <https://doi.org/10.1016/j.physbeh.2010.01.034>
- Rhoads, T.W., M.S. Burhans, V.B. Chen, P.D. Hutchins, M.J.P. Rush, J.P. Clark, J.L. Stark, S.J. McIlwain, H.R. Eghbalian, D.M. Pavelec, et al. 2018. Caloric restriction engages hepatic RNA processing mechanisms in rhesus monkeys. *Cell Metab.* 27:677–688.e5. <https://doi.org/10.1016/j.cmet.2018.01.014>
- Schonhoff, S.E., M. Giel-Moloney, and A.B. Leiter. 2004. Neurogenin 3-expressing progenitor cells in the gastrointestinal tract differentiate into both endocrine and non-endocrine cell types. *Dev. Biol.* 270:443–454. <https://doi.org/10.1016/j.ydbio.2004.03.013>
- Talchai, C., Xuan, S., Kitamura, T., DePinho, R.A., and Accili, D. 2012. Generation of functional insulin-producing cells in the gut by Foxo1 ablation. *Nat. Genet.* 44:406–412, S401. <https://doi.org/10.1038/ng.2215>
- Tan, Q., S.E. Akindehin, C.E. Orsso, R.C. Waldner, R.D. DiMarchi, T.D. Müller, and A.M. Haqq. 2022. Recent advances in incretin-based pharmacotherapies for the treatment of obesity and diabetes. *Front. Endocrinol.* 13:838410. <https://doi.org/10.3389/fendo.2022.838410>
- Thompson, C.A., A. DeLaForest, and M.A. Battle. 2018. Patterning the gastrointestinal epithelium to confer regional-specific functions. *Dev. Biol.* 435:97–108. <https://doi.org/10.1016/j.ydbio.2018.01.006>
- Tschöp, M., D.L. Smiley, and M.L. Heiman. 2000. Ghrelin induces adiposity in rodents. *Nature.* 407:908–913. <https://doi.org/10.1038/35038090>
- Tsuchiya, K., and Y. Ogawa. 2017. Forkhead box class O family member proteins: The biology and pathophysiological roles in diabetes. *J. Diabetes Investig.* 8:726–734. <https://doi.org/10.1111/jdi.12651>
- Weindruch, R., R.L. Walford, S. Fligiel, and D. Guthrie. 1986. The retardation of aging in mice by dietary restriction: Longevity, cancer, immunity and lifetime energy intake. *J. Nutr.* 116:641–654. <https://doi.org/10.1093/jn/116.4.641>
- Yamaza, H., T. Komatsu, S. Wakita, C. Kijogi, S. Park, H. Hayashi, T. Chiba, R. Mori, T. Furuyama, N. Mori, and I. Shimokawa. 2010. FoxO1 is involved in the antineoplastic effect of calorie restriction. *Aging Cell.* 9:372–382. <https://doi.org/10.1111/j.1474-9726.2010.00563.x>
- Yilmaz, O.H., P. Katajisto, D.W. Lamming, Y. Yilmatekin, K.E. Bauer-Rowe, S. Sengupta, K. Birsoy, A. Dursun, V.O. Giltman, M. Selig, et al. 2012. mTORC1 in the Paneth cell niche couples intestinal stem-cell function to calorie intake. *Nature.* 486:490–495. <https://doi.org/10.1038/nature11163>
- Yousefi, M., A. Nakauka-Ddamba, C.T. Berry, N. Li, J. Schoenberger, D. Bankler-Jukes, K.P. Simeonov, R.J. Cedeno, Z. Yu, and C.J. Lengner. 2018. Calorie restriction governs intestinal epithelial regeneration through cell-autonomous regulation of mTORC1 in reserve stem cells. *Stem Cell Rep.* 10:703–711. <https://doi.org/10.1016/j.stemcr.2018.01.026>

Supplemental material

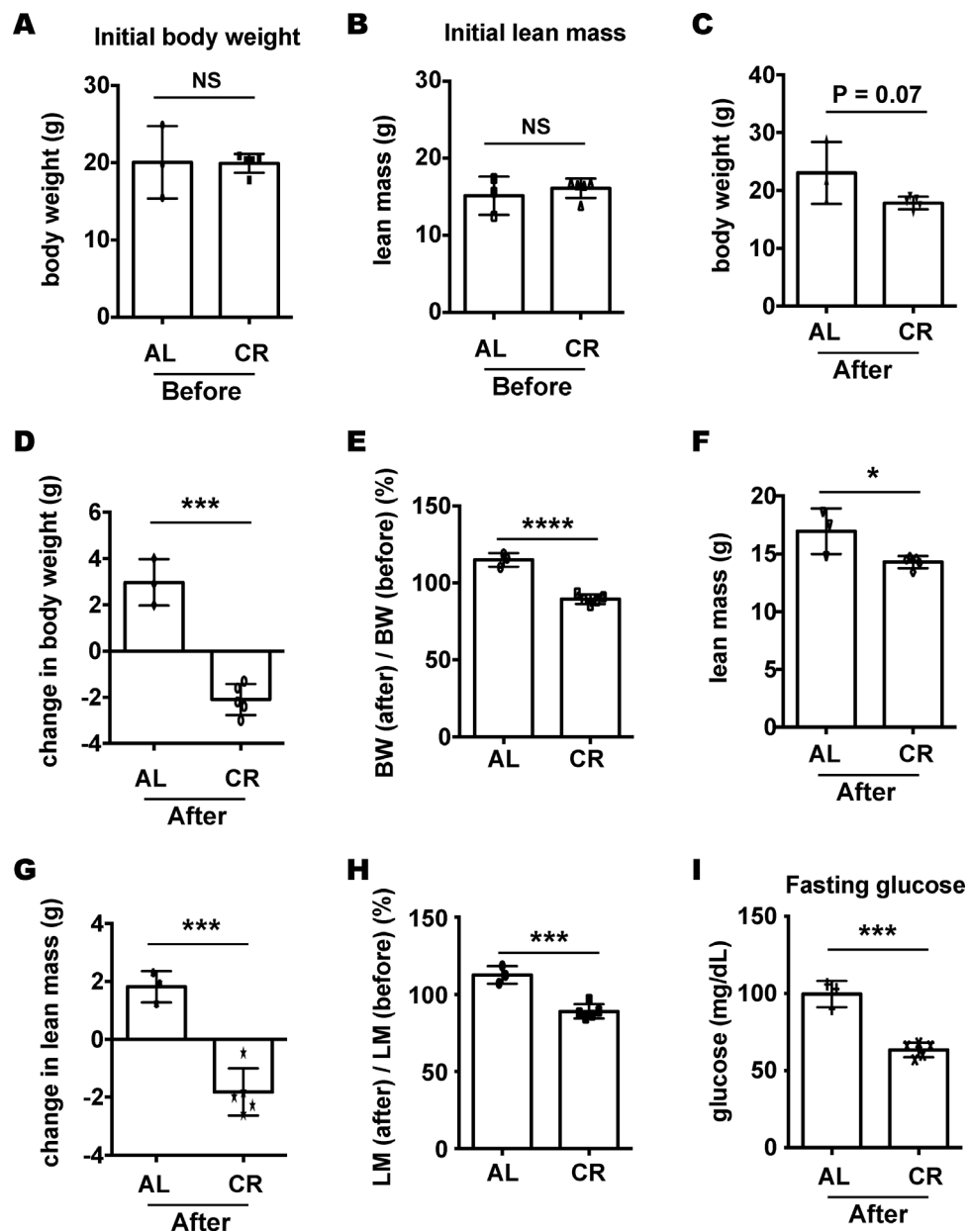


Figure S1. **Mice have lower body weight, lean mass, and fasting glucose levels after food restriction.** (A) Initial body weight (at 12 wk age) of female FOXO1-Venus (FoxV) reporter mice prior to food restriction. (B) Initial lean mass measurements (at 12 wk age) of FoxV mice prior to food restriction. (C–I) Measurements after FoxV mice were fed ad libitum (AL, $n = 3$ mice) or 30% food restricted (CR, $n = 5$ mice) for 4 wk. Data include: body weight (C), change in body weight calculated for each AL and CR mouse after 4 wk experiment (D), body weight (BW) displayed as percentage of initial weight (E), lean mass measurements (F), change in lean mass in AL and CR mice (G), lean mass (LM) displayed as percentage of initial mass (H), and blood glucose measurements after a 5 h fast in AL and CR mice (I). Bar graphs show mean \pm standard deviation. For all panels, each dot is an individual mouse. * $P < 0.05$, *** $P < 0.001$, **** $P < 0.0001$. NS = not significant.

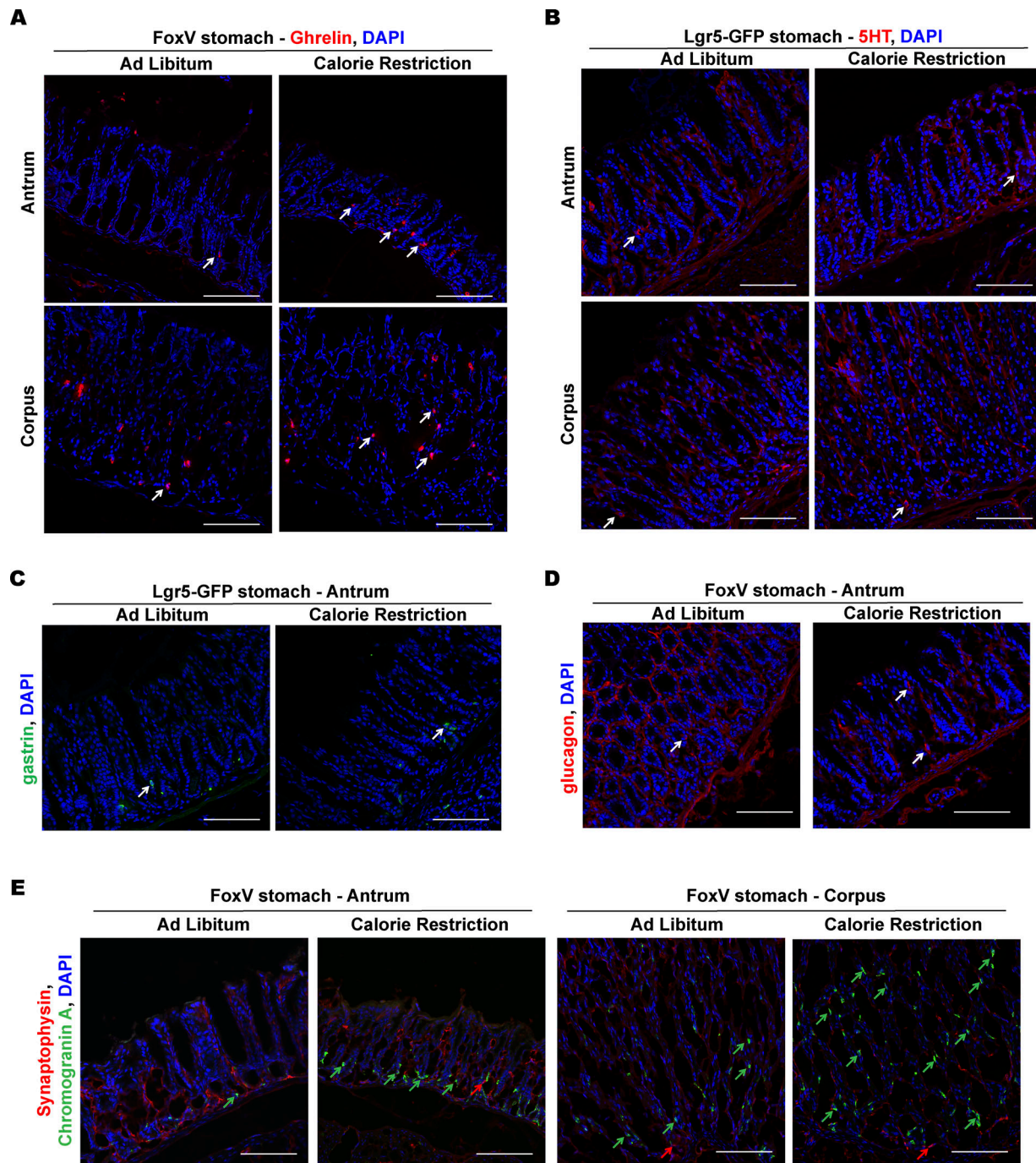


Figure S2. **Altered endocrine cell abundance in stomach tissue of female mice after calorie restriction.** (A–E) Representative fluorescent images of general and specific endocrine cell populations in stomach tissue from female FOXO1-Venus (FoxV) reporter mice calorie restricted (at 12 wk old) by 30% or fed ad libitum for 4 wk. Metabolic data for these mice are displayed in Fig. S1. Quantification of staining is also displayed in Fig. 1. White, green, and red arrows denote immunoreactive cells for respective markers. Scale bar is 100 μ m. DAPI counterstains nuclei.

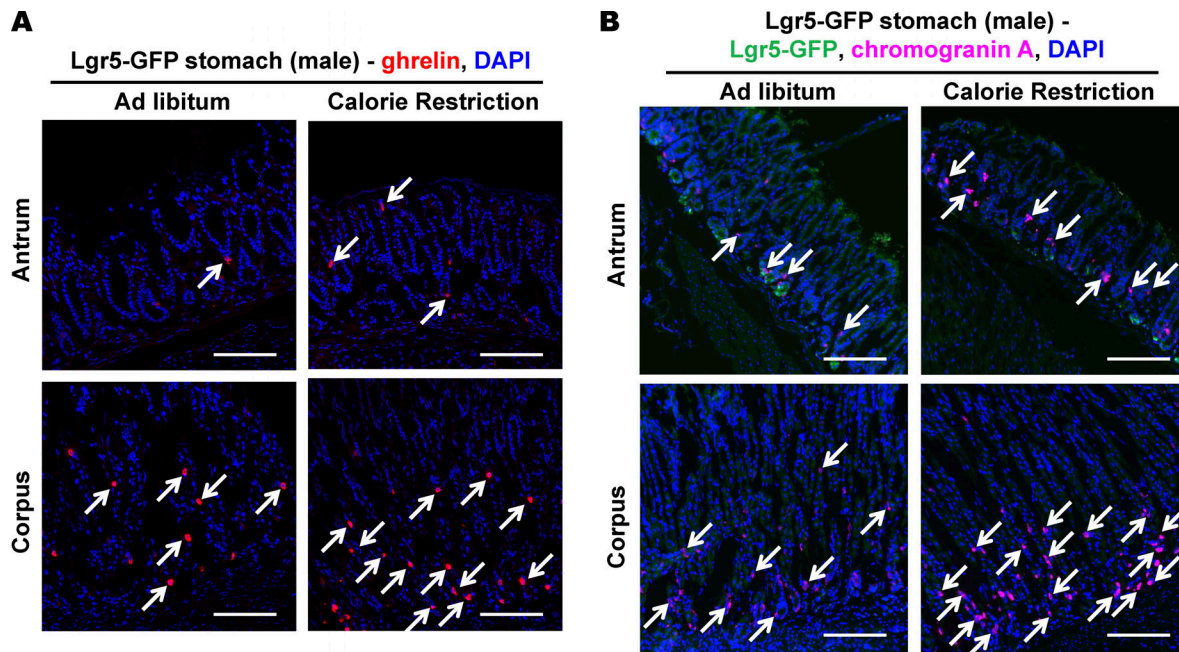


Figure S3. **Altered endocrine cell abundance in stomach tissue of male mice after calorie restriction.** (A and B) Representative fluorescent images of ghrelin+ (A) and chromogranin A+ (B) cells in the indicated stomach tissue from male Lgr5-GFP reporter mice fed ad libitum or 30% calorie restricted for 4 wk. Mice were 14–16 wk old at the start of calorie restriction. Metabolic data for these mice are displayed in Fig. 3. Quantification of cell populations are displayed in Fig. 1. White arrow denotes positive cell. Scale bar is 100 μm. DAPI counterstains nuclei.

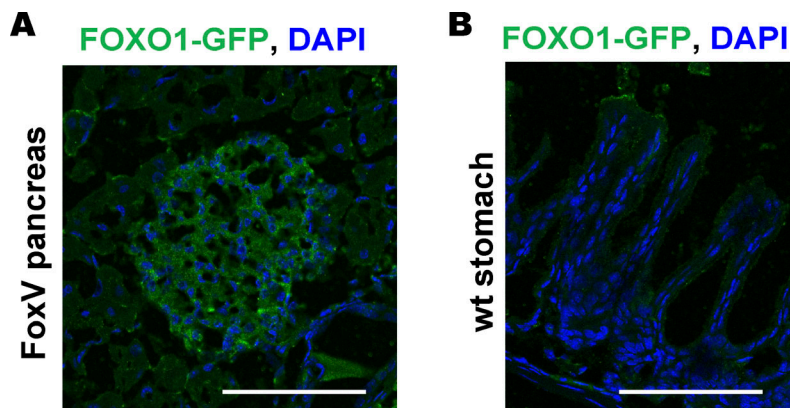


Figure S4. **Using FOXO1-Venus reporter mice to detect FOXO1+ cells.** (A) Pancreatic tissue from FOXO1-Venus reporter mouse (FoxV) stained for GFP (which recognizes Venus reporter). This represents a positive control for GFP staining. (B) Wild-type (wt) antral stomach tissue stained from GFP showing no positive signal in stomach tissue lacking FoxV reporter. White scale bar is 100 μm. DAPI counterstains nuclei.

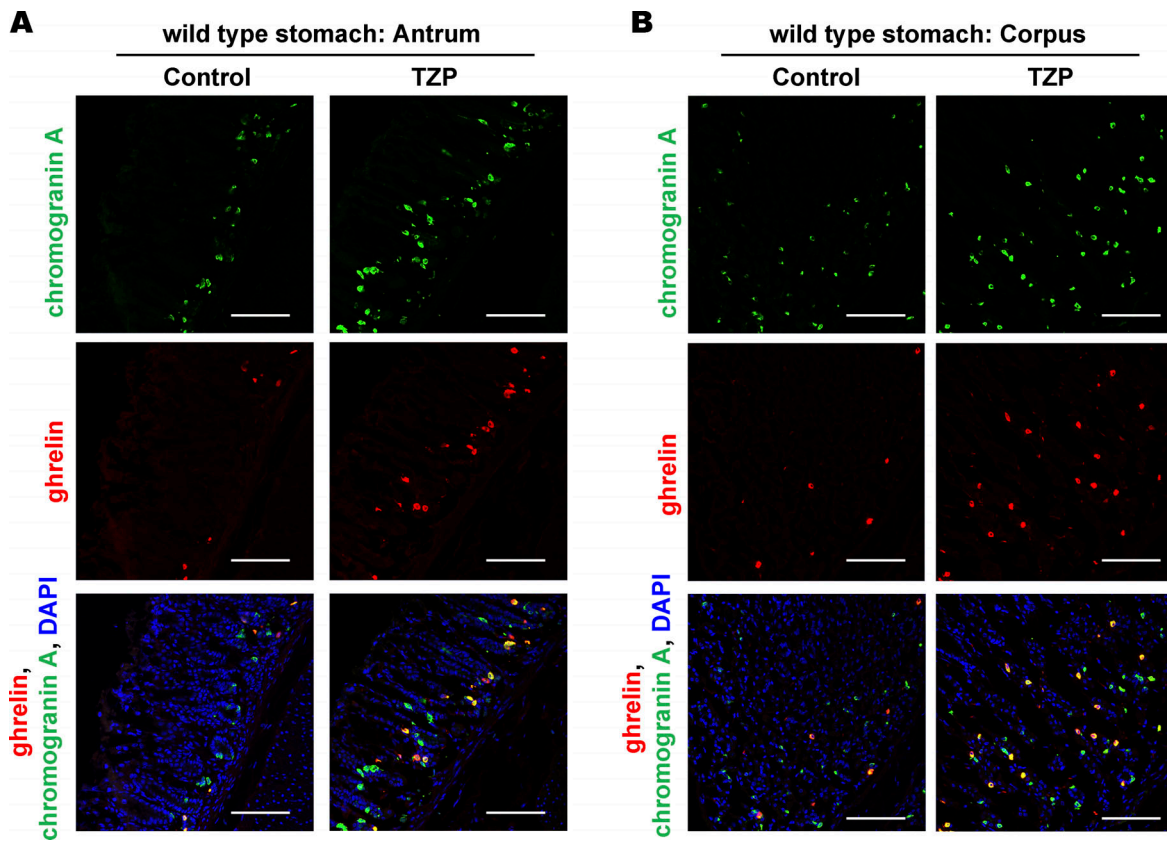


Figure S5. **Increased endocrine cell abundance in stomach tissue from mice after treatment with tirzepatide (TZP).** (A and B) Representative fluorescent images of ghrelin+ and chromogranin A+ cells in the antrum (A) and corpus (B) stomach from male wild-type mice (13 wk old) treated daily with 30 nM/kg TZP for 5 days. Metabolic data and quantification of cell populations are displayed in Fig. 7. Scale bar is 100 μ m. DAPI counterstains nuclei.